The Thesis committee for Daniel Patrick Pinkston

Certifies that this is the approved version of the following thesis:

From Outcrop to Functional Reservoir Model – Using Outcrop Data to Model the Tidally Dominated Esdolomada Sandstone, NE Spain

APPROVED BY SUPERVISING COMMITTEE:

Supervisor:

Ronald Steel

Lesli Wood

Cornel Olariu

From Outcrop to Functional Reservoir Model – Using Outcrop Data to Model the Tidally Dominated Esdolomada Sandstone, NE Spain

by

Daniel Patrick Pinkston, B.S. Geo. Sci.

Thesis

Presented to the Faculty of the Graduate School

of the University of Texas at Austin

in Partial Fulfillment

of the Requirements

for the Degree of

Master of Science in Geological Sciences

The University of Texas at Austin

May 2012

Acknowledgements

I would like to give a big personal thanks to Manasij Santra for helping me with the use of Schlumberger's Petrel software in the modeling portion of my thesis. Without his knowledge and expertise, I can confidently say I would not have been able to complete this undertaking. I would also like to thank my advisor, Ronald Steel, for his patience and guidance throughout the last year of my Masters. Thank you to Lesli Wood for sparking my interest in sedimentology and sand bar systems, and for her edits and input on my thesis. Thank you to Cornel Olariu for his assistance in the field and in the office. Thank you to Iulia Olariu for her help doing field work in Spain and for letting me find ample use in referencing her paper on the lower Esdolomada 1 sandstone. Thank you to my friend, Kain Michaud, who was my field partner and cliff scaling competitor while measuring sections in Spain. One final thanks goes to William Burnett, my friend and roommate throughout grad school, for his generosity and camaraderie.

Abstract

From Outcrop to Functional Reservoir Model – Using Outcrop Data to Model the Tidally Dominated Esdolomada Sandstone, NE Spain

by

Daniel Patrick Pinkston, M.S. Geo. Sci.
The University of Texas at Austin, 2012

Supervisor: Ronald Steel

The Esdolomada Sandstone member 2 crops out in the Tremp-Graus Basin of north-central Spain and forms the uppermost part of the Eocene Roda Formation. The second Sandstone unit within the Esdolomada member (ESD2) consists of bioturbated and shell-rich, very-fine sandstones as well as stacked sets of fine- to coarse-grained cross-stratified sandstones. The overall upward trend in the member is commonly upward thickening and coarsening of beds into and through the cross-stratified interval, though at some few locations there is no obvious trend or even upward thinning of beds. The internal architecture of the member is one in which groups of beds lie between master surfaces that dip

highly obliquely to the migration direction of the individual cross strata. The ESD2 is interpreted to be a shelf tidal sand bar within the overall transgressive Esdolomada Sandstone member. It is likely that these bars migrated in a coast parallel fashion, as suggested by the cross-bed orientations, but also accreted laterally away from the coast along the seaward-dipping master surfaces. LIDAR (light detection and ranging) data collection for the Esdolomada member was attempted along the Isábena River near the village of Roda de Isábena, with a total lateral coverage of approximately 3 kilometers. Detailed outcrop measurements were made in accessible areas along the same transect.

Outcrop analogs are the best source of data to understand reservoir heterogeneities and to build reservoir analogs for fluid flow simulations. Sand-rich, offshore tidal sandbodies are usually surrounded by marine mudstones, and are recognized from their very orderly stacking of cross-stratified sets (more orderly than in fluvial settings) , their complex internal architecture of master surfaces dipping obliquely to the direction of migration of the contained cross strata and their significant sandstone/mudstone heterogeneities. Tidal bar systems such as the ESD2 are appealing hydrocarbon prospects for several reasons. Primarily, they are relatively coarse grained, have a high degree of lateral continuity, and are relatively clean sands. In places where sand beds are stacked, they create enough thickness to offer good vertical permeability; however, mud-draped cross-beds can create heterogeneities in this type of system that buffer fluid flow.

Due to a fairly unsuccessful attempt to obtain LIDAR coverage of the ESD2, in order to build an analog reservoir model, surfaces were instead based on measured sections and outcrop photomosaics. Using Schlumberger's Petrel software, facies logs were created from measured section data, and then interpolated to make a facies and porosity model.

Table of Contents

List of Tables

List of Figures

Chapter 1: Introduction and Goals of Study

Mud Layer Heterogeneity

Reservoir models are a frequently utilized tool when targeting oil and gas plays for exploitation and the geological heterogeneities are the key factor for an accurate description of the reservoirs (Jackson et al., 2005, 2009; Pringle et al., 2006, White). The geologic models provide a 3-D visualization of the distribution of reservoir properties, which allows geologists and engineers to target optimal zones for production. For most reservoir models, petrophysical properties from log data are interpolated between wells and geometries are based on seismic data. These techniques often fail to capture the level of complexity found in many geologic systems. Increasingly, outcrop data is being used to generate analog reservoir models, similar to systems found at depth. Outcrop data allows for finer scale interpretation of surfaces, grain size, petrophysics, etc. when compared to seismic and well log data, and hence a better, more accurate model can be built from this data.

Tidal bar sandstone reservoirs (Wood, 2004), the study choice in this work, can be very heterogeneous and may contain many possible barriers to fluid flow, most of these at an inter-well and sub-seismic scale (Brønlund, 2010). Creating an analog reservoir model based on outcrop data allows for a unique opportunity to circumvent some of the shortcomings in the traditional method of reservoir modeling.

The possible barrier-to-flow heterogeneities, usually at inter-well scale, that can be encountered in Tidal Bar Sandbodies are usually mudstones in various shapes and forms, irrespective of whether they originate from a single tidal cycle, from groups of Neap or Spring tidal cycles, or from seasonal or longer term accumulations of muds. The most common cases of mud include the following, taken from good examples at different global localities:

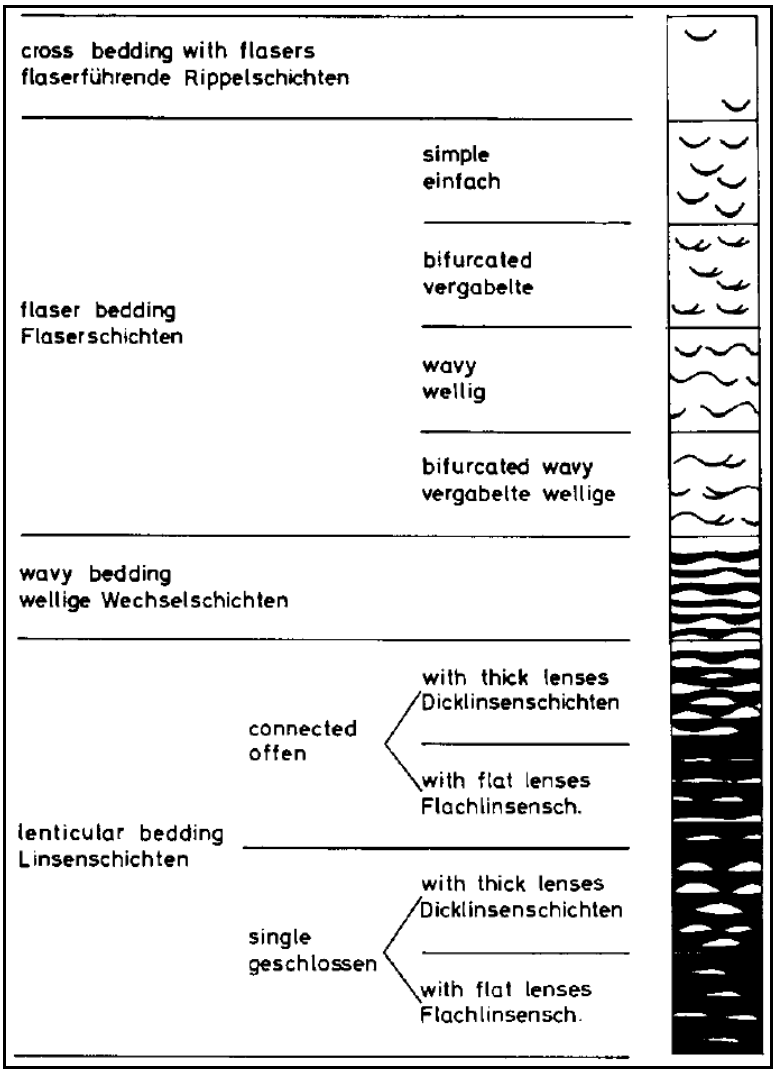

Figure1: Classification of tidal deposits (flaser and lenticular bedding) from Reineck and Wunderlich, 1968.

1. Mud drapes in ripple-laminated sandstones, the classic flaser bedding, has very thin (mm to cm) and very short length (discontinuous cm to dms length) mud laminae (Figure 2).

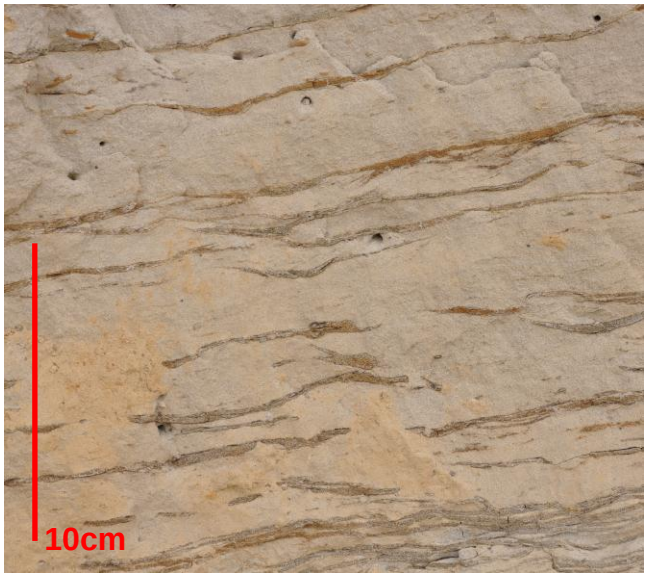

Figure 2: Discontinuous mud drapes filling ripple troughs.

2. Thin (<0.5cm) mud drapes on the foresets/toesets of individual cross-stratified sets (dunes), with a frequency equivalent to half a tidal cycle (ca. 6 hrs). Such drapes become thicker during bundling of Spring Tide foresets. These mud drapes would commonly extend for 10s of cm to 10s of meters (Figure 3)

Figure 3: Thin mud draping foresets of a cross-stratified sandstone.

3. Thicker mud layers, usually amalgamated mud layers with some thin siltstone interbeds, occur as extensive sub-horizontal muddy beds separating sandier intervals within the tidal bar succession (Figure 4). These thicker muddy units would have accumulated over longer time intervals than above, but can be seasonal (winter-summer), or of even longer duration. They are thicker (cm to 10 cm) and more extensive (10s of meters to 100s of meters) than the above.

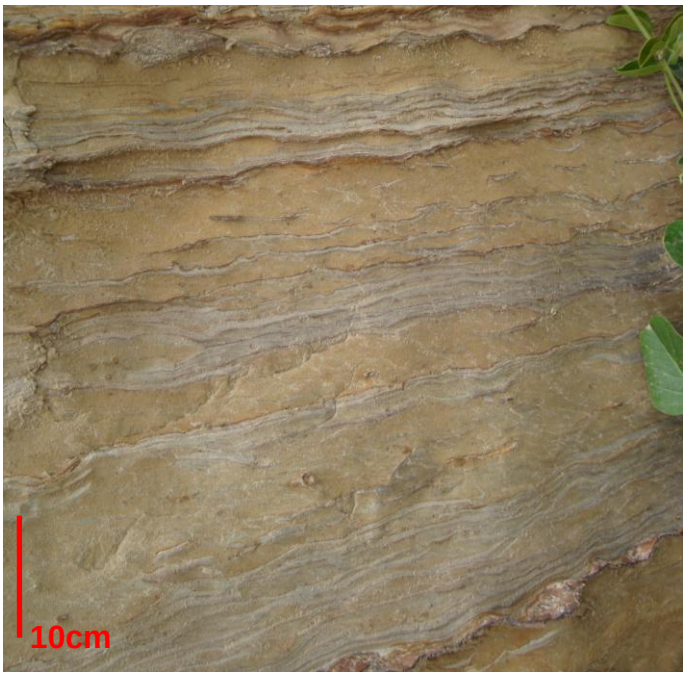

Figure 4: The muddy intervals are ca. 10cm thick, separating sandy intervals.

4. In addition to these discrete mud-layer heterogeneities in typical Tidal Bar reservoirs, there occur also heterogeneity caused simply by bioturbation (Figure 5). Ironically the bioturbation, caused by a thorough mixing of discrete sand and mud layers, can also provide better flow properties than it would have been prior to bioturbation.

Figure 5: Very bioturbated sandstone. This will reduce reservoir quality in a clean sand reservoir, but may enhance quality in a mud-sand layered reservoir.

Goals of Study

The goal of this study is to describe the facies and geometry of a tidal bar sandstone unit from the Esdolomada Sandstone of northern Spain, and to use outcrop based modeling to create an analog reservoir model for this tidal bar system. We hypothesize that reservoir simulation of tidal bars can be improved through integration of quantitative and qualitative outcrop data into the process. The following chapters will discuss previous work done in the area, a regional overview, geology of the study area, methods used to collect the data, and discussion of the tidal bar data, and then the methods and results of modeling the Esdolomada 2 sand bar.

Chapter 2: Geologic Overview

Structural Setting

The object of this study, the Esdolomada Sandstone member of the Roda Formation, crops out along the Isábena River valley in northern Spain, is Eocene in age, and was deposited in the Tremp-Graus Basin in the southern Pyrenees. The Tremp-Graus Basin is a foreland basin, oriented WNW-ESE (Tinterri 2007), and is one of a series of piggyback basins located atop the Monsec thrust sheet. The Monsec thrust is one of three associated compressional fronts that include the Boixols and Sierra Marginales thrusts that spread south during the Cretaceous (see Figure 6 below).

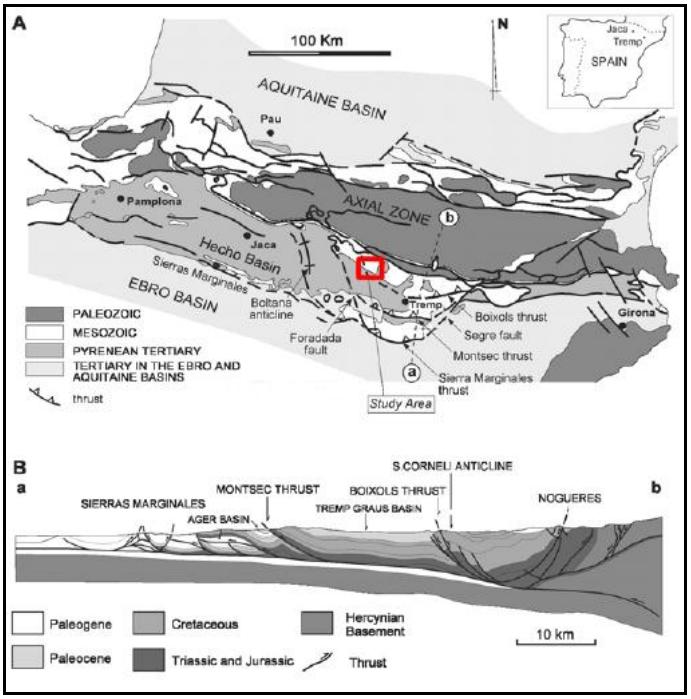

Figure 6: Regional geologic map (A) and cross section (B) containing the Tremp Grauss basin with field area shown in red box (modified from Tinterri 2007).

Stratigraphic Setting

The succession of interest is the Ager Group, named by Mutti the Figols Group (Figure 7), which is divided into six unconformity-bound sequences that are interpreted to record a syntectonic basin filling phases, each of which has an overall shallowing upward character (Tinterri 2007). The Roda Formation lies directly above the Puebla de Roda Limestone of the Tremp-Ager Group, and below the carbonate deposits of the Morillo Limestone (Figure 7).

The Figols group was deposited following the creation of two subsiding basins associated with a contractional phase along the nearby thrust front, and represents the first basin wide distribution (in both basins) of Eocene siliciclastics above Paleocene transgressive shallow marine carbonates.

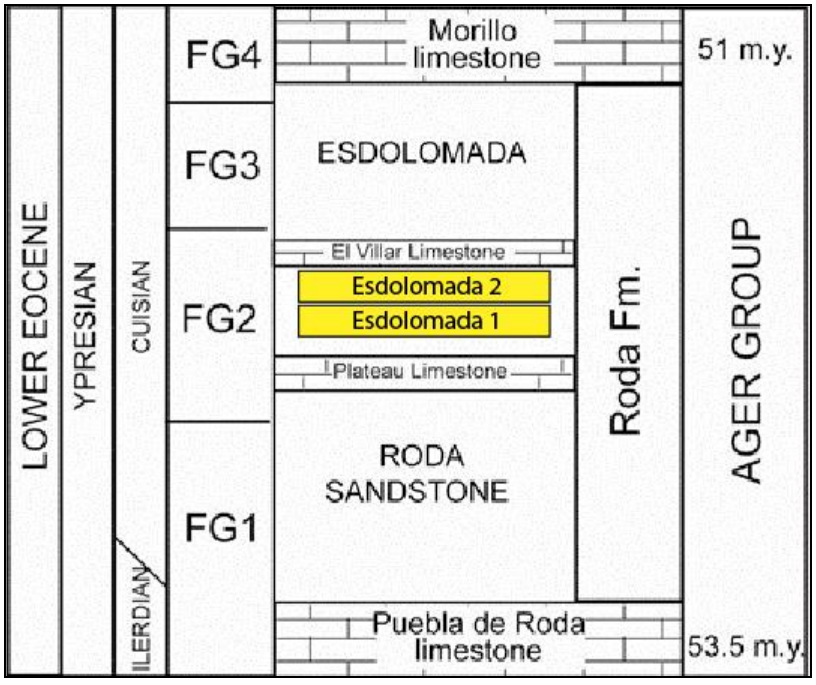

Figure 7: Stratigraphy of the Esdolomada sandstone and surrounding geologic units (modified from Tinterri 2007).

The Figols group is up to 1200m thick and can be divided up into four stratigraphic units (FG1-FG4) bounded by angular unconformities. These four groups record an overall shallowing upward trend related to the southward movement of the Boixols and Montsec thrusts and resultant progradation of fluvio deltaic systems. The entire Figols Group was deposited over 2.7Ma and each subdivision has been interpreted to include a falling-stage to lowstand regressive systems tract generated from the propagation of the thrusts followed by coastal transgression during a relative rise in sea level due to tectonic subsidence. Each of the subdivisions represents a 3rd-order cycle, and each is manifested as a basal regressive shallow marine sandstone wedge overlain by a transgressive carbonate facies and a capping a highstand mudstone.

In the Isábena River valley, an angular unconformity marks the bottom of the Figols Group. Above this is FG1, which contains thick shelfal/slope mudstones with thin delta-front sandstone lobes overlain by the Puebla de Roda Limestone. Above the limestone is mostly mudstone and a laterally continuous bioclastic (storm) bed, that signifies the transition to predominantly fluvio-deltaic deposits of the Roda Formation.

The Roda Formation, interpreted as a river-dominated delta system, is described as consisting of six fluvio-deltaic conglomeratic sandstone units (R1-R6) (Figure 8), that individually prograde but have an overall basinward-stepping stacking pattern. Each contains a basal sandstone wedge capped by a siltstone and mudstone (Lopez-Blanco et al., 2003). Strong seaward progradation

produced characteristic meter to decimeter scale clinoforms within the Roda units. The lack of wave-generated signals suggests that it was strongly fluvial influenced. The overlying strata of concern (Esdolomada Member) show a backstepping trend, making the Roda-Esdolomada succession to be a single, very large-scale regressive-transgressive clastic wedge (Figure 8).

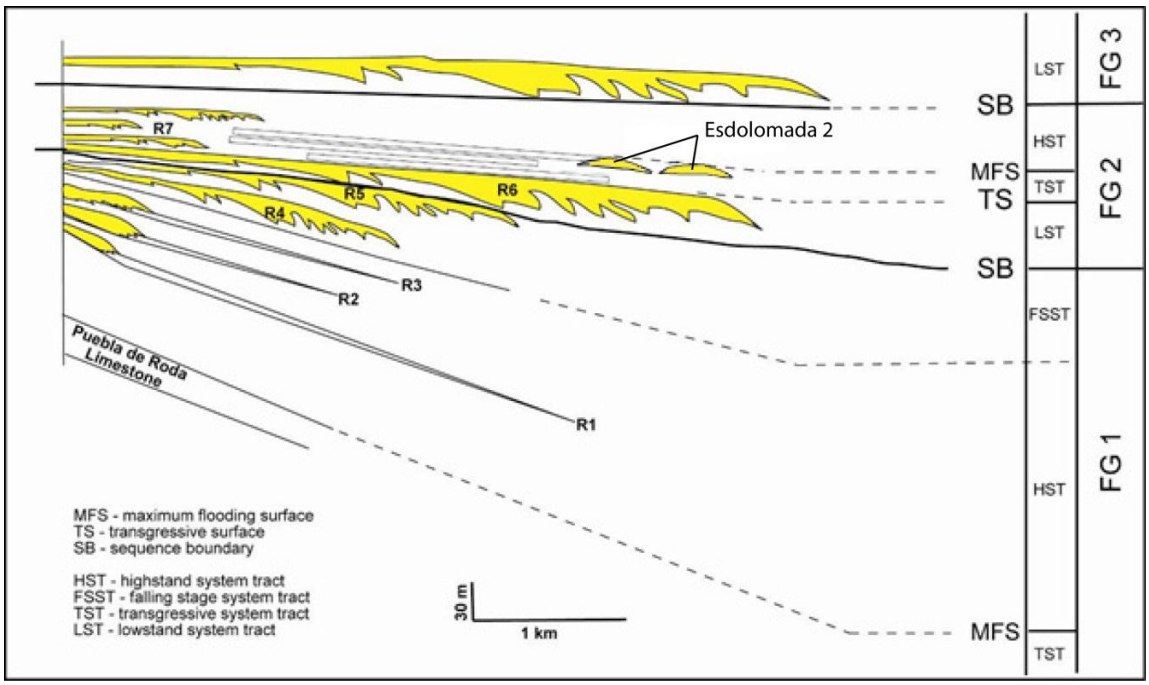

Figure 8: Sequence stratigraphic representation of Figols Groups 1-3, with the location of the Esdolomada 2 indicated (modified from Tinterri 2007).

The Esdolomada and Roda clastic wedge is believed to have been built synchronously with tectonic activity along the Montsec thrust (Tinterri 2007). Abundant soft sediment deformation within the Roda, but pronounced absence within the Esdolomada, suggests there was a lull in tectonic activity during the

development of the transgressive Esdolomada Member deposition. Underlying the Esdolomada member is the Plateau Limestone, which is a bioclastic grainstone. Sandwiched between the Plateau limestone and the Esdolomada is a heavily bioturbated calcareous mudstone with abundant marine fauna that is referred to as a 'storm bed' (Tinterri 2007) and serves as a good regional marker. Above the storm bed are several meters of fine grained bioturbated sandstones and then six meters of medium grained, cross-stratified sandstone sets that make up the first sand bench of the Esdolomada member (ESD1). Above ESD1 is a medium-grained sandstone with extremely abundant foraminifera and *Thalassinoides* burrows that has been interpreted to represent a marine hardground, probably a transgressive surface and this is overlain by the second Esdolomada sandstone bench (ESD2), the object of study in this thesis.

The ESD2 contains plentiful examples of medium to fine grained stacks of cross strata, some mud draped, suggesting a strong tidal influence. This deposit has been interpreted to be an elongate tidal bar that was migrating in a direction oblique to the dominant paleocurrent direction, as evidenced by a discrepancy between the dip direction of smaller cross beds and the larger scale master surfaces of the sandstone unit.

Chapter 3: Field Methods

Vertical Sections

Vertical sedimentological sections were measured up through the Esdolomada 2 sandbody at intermittent locations along a roughly 3km transect through the Isábena River valley. A total of 10 measured sections were gathered along this transect (Figure 10). Paleocurrent data was recorded wherever possible for each measured section (summarized in Table 2), and photomosaics were created for well exposed sections of the outcrop. The series of measured sections contain important geologic data including thickness, lithology, grain size, paleocurrent data, bedding scale and character, and trace fossils. An example measured section is shown on the following page.

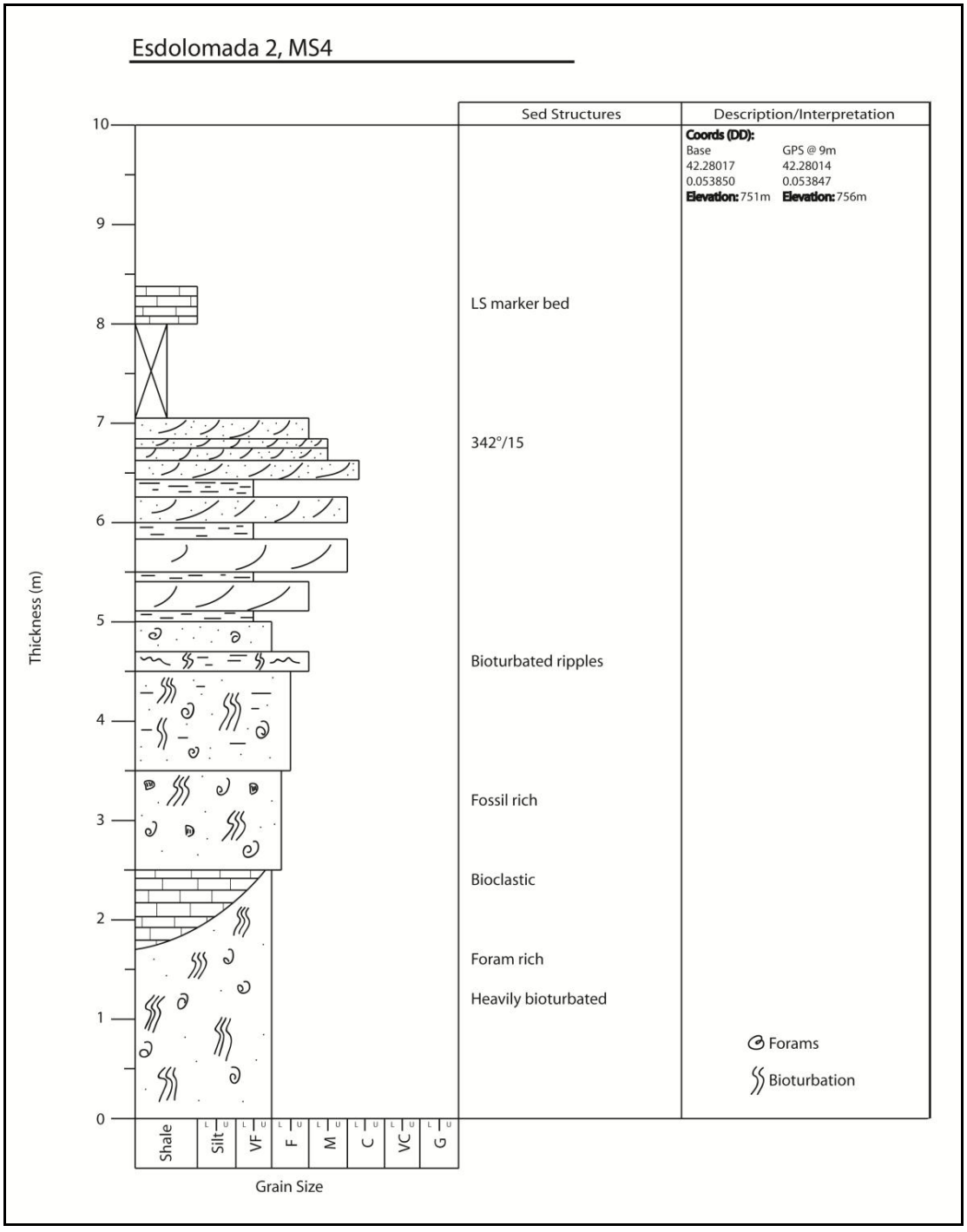

Figure 9: Example of a vertical sedimentological profile through ESD2.

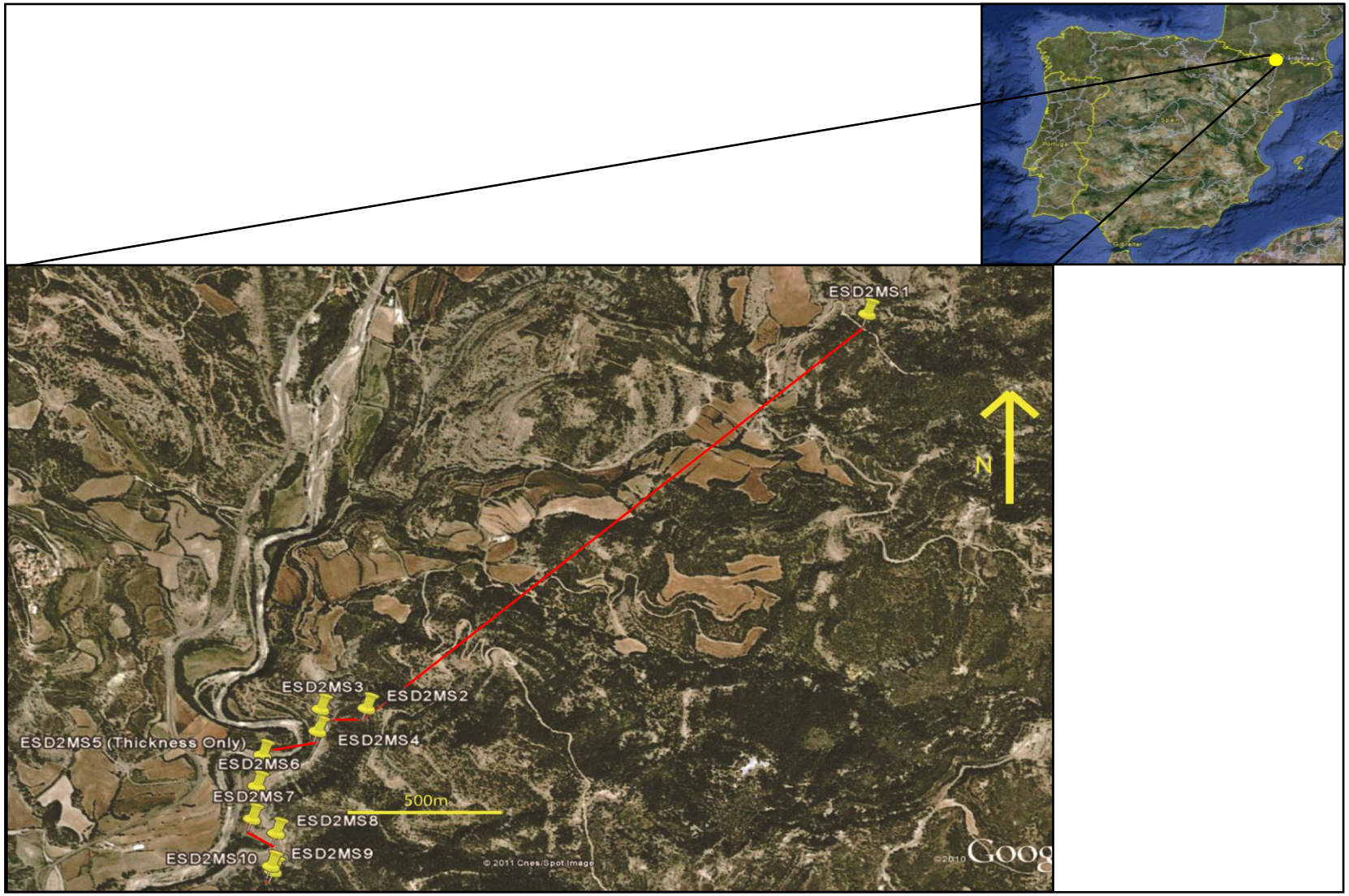

Figure 10: Outcrop locations where the 10 vertically measured sections were made along Isábena River valley. See the measured section and interpretation on Figure 14.

The Esdolomada 2 example section is characterized by muddy, very fine grained fossiliferous sandstones and siltstones that pass upwards to fine grained, stacked sets of crossbedded sandstones that become more uniformly sorted towards the top of the section. The mud content decreases from the bottom to the top of the section, as the cross strata become thicker. The crossbedding, represents migrating subaqueous dunes, but the cross-bed direction is noticeably oblique to the orientation of a series of master surfaces that pass down through the body from top to bottom. This indicates that the strongest tidal currents were flowing to the NW, whereas the sandbody itself was accreting to the southwest as shown by the orientation of the master surfaces. All of the individual measured sections are included in the appendix at the end of the thesis. Figures 11 and 12 show the measured sections within the context of broader outcrops of the Esdolomada.

Photomosaics

Photomosaics of well exposed outcrop were taken where possible. In several cases, photomosaics include measured section locations (see figures 11 and 12 below). The ESD2 member is located on a steep hillside that is heavily vegetated, making capturing good examples of the outcrop difficult in many places. The ESD2 in Figure 11 is in a relatively proximal position, in a paleogeographic context. It contains stacked planar cross strata and finer, bioturbated sands at its base. The overall character is of a blocky sand, which is typical of a bar deposit. Total thickness is 8.4m. Figure 12 shows the ESD2 in a

more distal location, and displays some observable trends versus the distal location. For example, the blocky crossbedded sands at the top are thicker in the distal section and lack the finer grained beds in between that occur in the proximal section. In addition, there is a greater abundance of crossbedded strata in the distal section and noticeably less bioturbation. The heavily cemented bioclastic bed is absent from the distal section, and the overall thickness of the section indicates the bar is thinning distally.

	Crossbeds			Master Surfaces	
Measured Section	Azimuth	Dip		Azimuth	Dip
ESD2MS1	198	23		213	9
ESD2MS3	360	9			
	351	15			
	339	18			
	350	9			
	340	19			
	348	20			
	360	20			
ESD2MS4	342	15			
ESD2MS6	338	12			
	27	22			
ESD2MS7	342	40			
	342	24			
	351	20			
	8	22			
	336	28			
	340	21			
	318	17			
ESD2MS8	72	19			
	83	22			
	320	12			
	354	13			
	314	12			
	340	18			
	328	13			
	338	13			
	340	14			
	310	17			
ESD2MS9	330	15		175	20
ESD2MS10	340	5		220	5
	312	10		223	10
	303	10		210	6
	290	15			
	300	9			
Average	296	16.794		208.2	10

Table 1: Paleocurrent data from measured sections for crossbeds and master surfaces with their averages at the bottom.

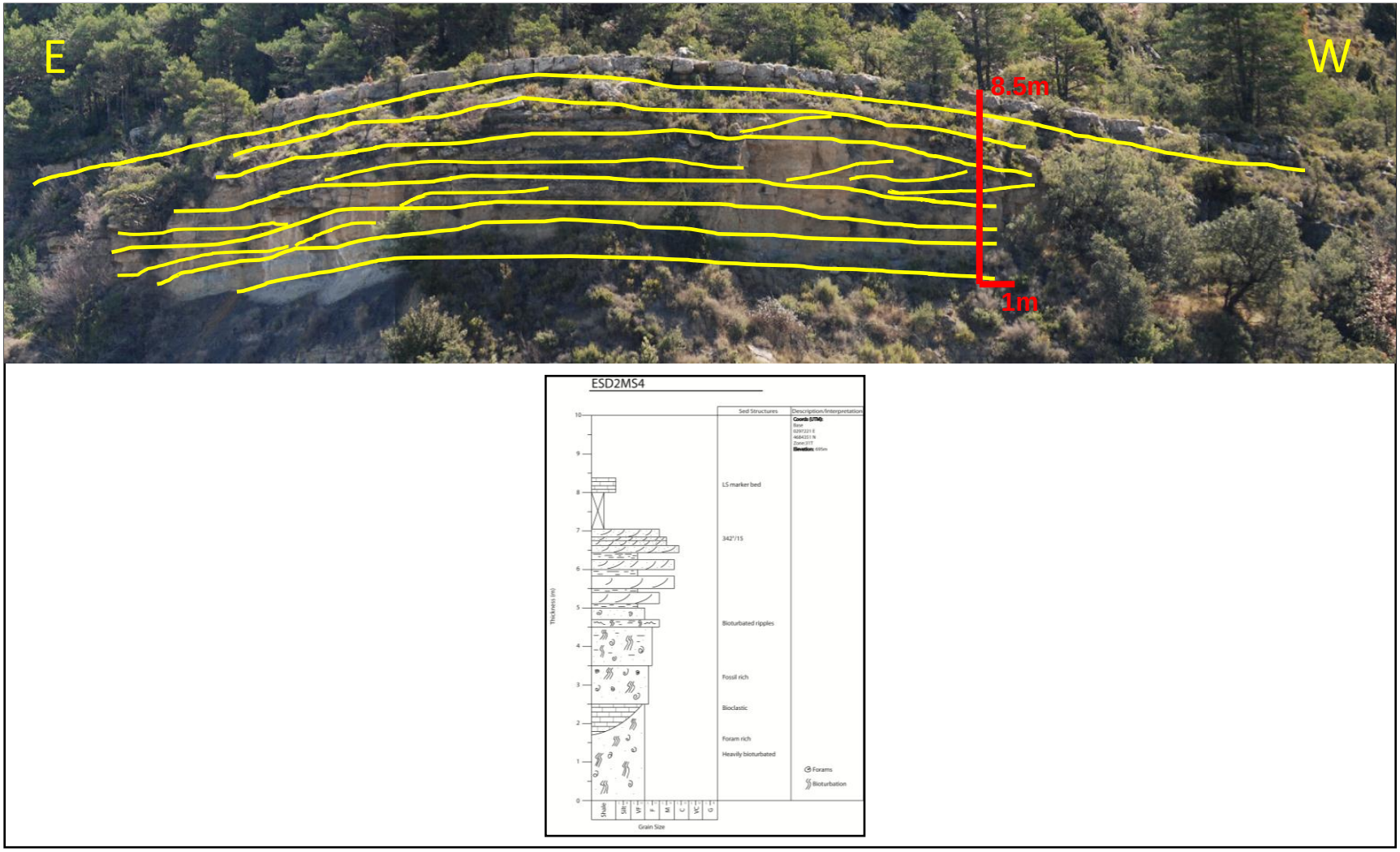

Figure 11: Photomosaic of ESD2 sandstone from a proximal location, with bedding planes and crossbedding highlighted in yellow. The measured section taken in this location is indicated by the vertical red line and shown below the photomosaic.

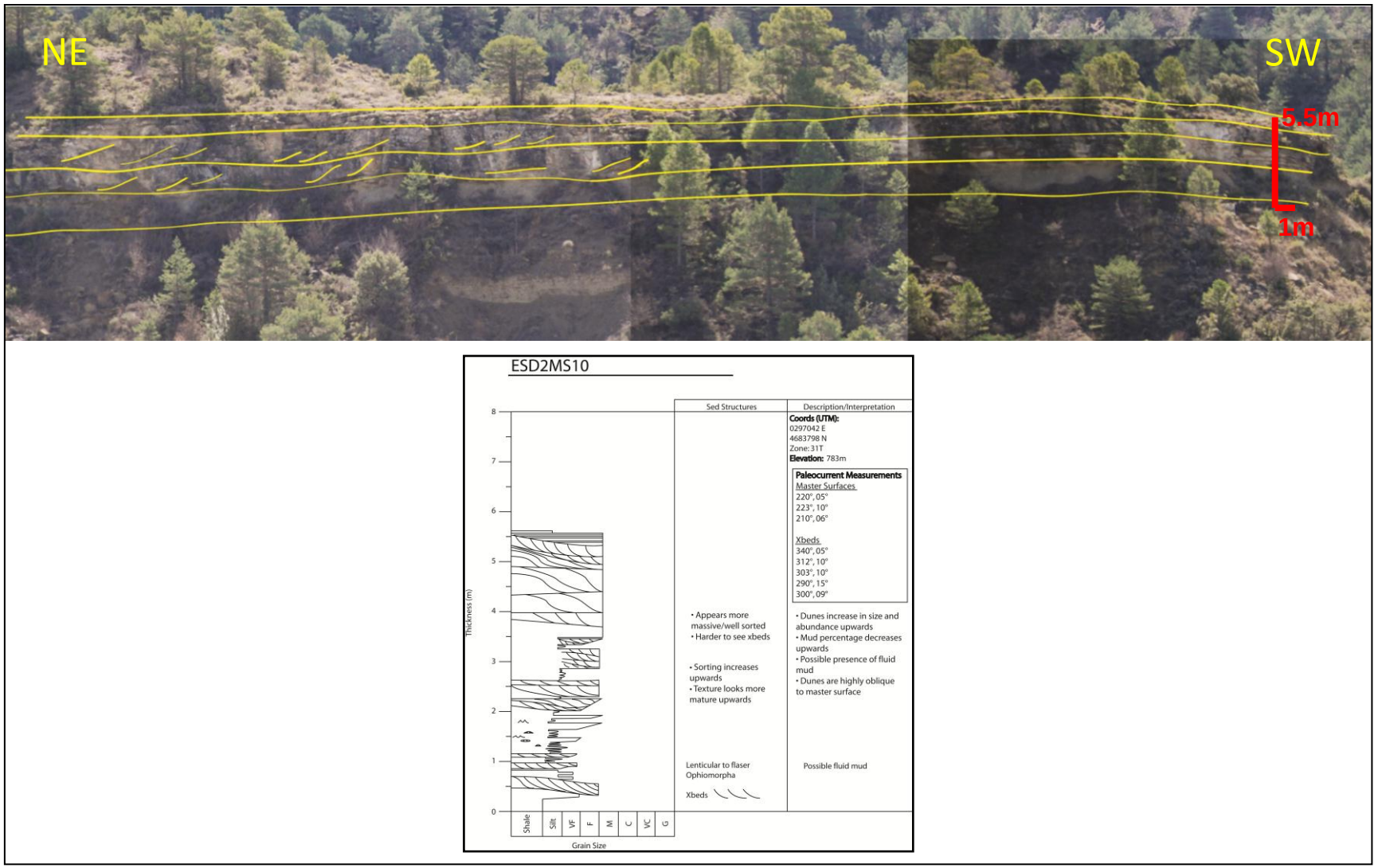

Figure 12: Photomosaic of the ESD2 sandstone from a distal location (about 400m), with bedding planes and crossbedding highlighted in yellow. The measured section taken in this location is indicated by the vertical red line and shown below the photomosaic.

Chapter 4: Results – Geologic Model

Facies

For the sake of creating a 2D model, 5 specific facies, based on the variability within the measured sections, were designated to capture the level of geologic heterogeneity found in a tidal bar system. The facies are listed and described below:

1. Fine to medium-grained cross bedded sandstone

   The bulk of the tidal sand bar is composed of fine to medium-grained crossbedded sandstone sets that average 40-50cm in thickness between master surfaces. The parallel sided character of the set boundaries and the lack of ‘smiley faces’ strongly suggests that the cross-bedded sets are planar, i.e. generated from 2D dunes. Crossbed sets stack into packages of up to 5-7m in thickness. The foresets are relatively high angle, with an average slope of up to 20 degrees depending on how the surface of the outcrop intersects them. When the outcrop surface parallels the primary current direction, the crossbeds appear as high angle sigmoidal beds. There are a variety of types of trace fossils sparsely present within the crossbed sets, including *Thalassinoides*, *Skolithos*, *Machronichnus*, and *Psilonichus*. The stacked large (40-50 cm) thick cross-strata indicate a high energy environment with strong currents forming subaqueous dunes. Mud

drapes on the crossbeds are common, suggesting a tidal environment in which the slackwater period was long enough in duration to allow mud to settle out of suspension and the subsequent ebb tide was weak enough to preserve some of the mud drapes. The trace fossils observed are characteristic to marine environments (*Skolithos* ichnofacies).

2. Basal silty sand

   This is found at the base of the Esdolomada 2 sandbody i.e., along the toes of the downlapping master surfaces. This sandstone is fine grained and contains occasional plane parallel bedding in places where bioturbation hasn't destroyed primary structures. Trace fossils are common and include *Planolites*, in addition to the aforementioned traces in the crossbedded sand facies. The degree of bioturbation is significant. The thin bedded character of the facies and the abundant mud indicate a low energy environment. The trace fossil assemblage suggests an environment with marine salinities while the high intensity of the bioturbation indicates relative low sedimentation rates.

3. Heavily cemented bioclastic sand

   Also referred to as a hardground, this sandstone is heavily carbonate cemented and composed mainly of foraminifera and mollusk fragments. It is laterally persistent and works well as a

marker bed. Its thickness is fairly uniform and ranges from 30-50cm. Bioturbation has destroyed any primary structures, but the preserved *Thalassinoides* burrows indicate a *Glossifungites* ichnofacies. Within a sequence stratigraphic framework, this facies would be a maximum flooding surface at the top of the Esdolomada 2. This facies indicates a very low sedimentation rate and probably a deepening of the water.

4. Planar laminated, alternating mudstones and thin sandstones

   Moderately bioturbated, thinly planar laminated (5-15cm scale) mudstone and sandstone. This facies occurs between the cross bedded sandstone facies as either a mudstone or as a heterolithic fine grained sandstone. The thin bedded character of the facies indicates the low energy and the alternation with the cross bedded sandstone denotes a presence of areas with lower energy between dunes, or alternatively times when the entire dune fields were abandoned.

5. Heavily bioturbated sandstone

   Heavily bioturbated, fine to v.fine-grained sandstone with abundant foraminifera, echinoids, and mollusk fragments. Common trace fossils include *Thalassinoides*, *Skolithos*, *Machronichnus*, and *Psilonichus*. No bedding is present, and the pervasive bioturbation suggests that energy levels and sedimentation rates were low and

according to the abundance of fossil fragments this was most likely a shelf environment with normal marine salinities.

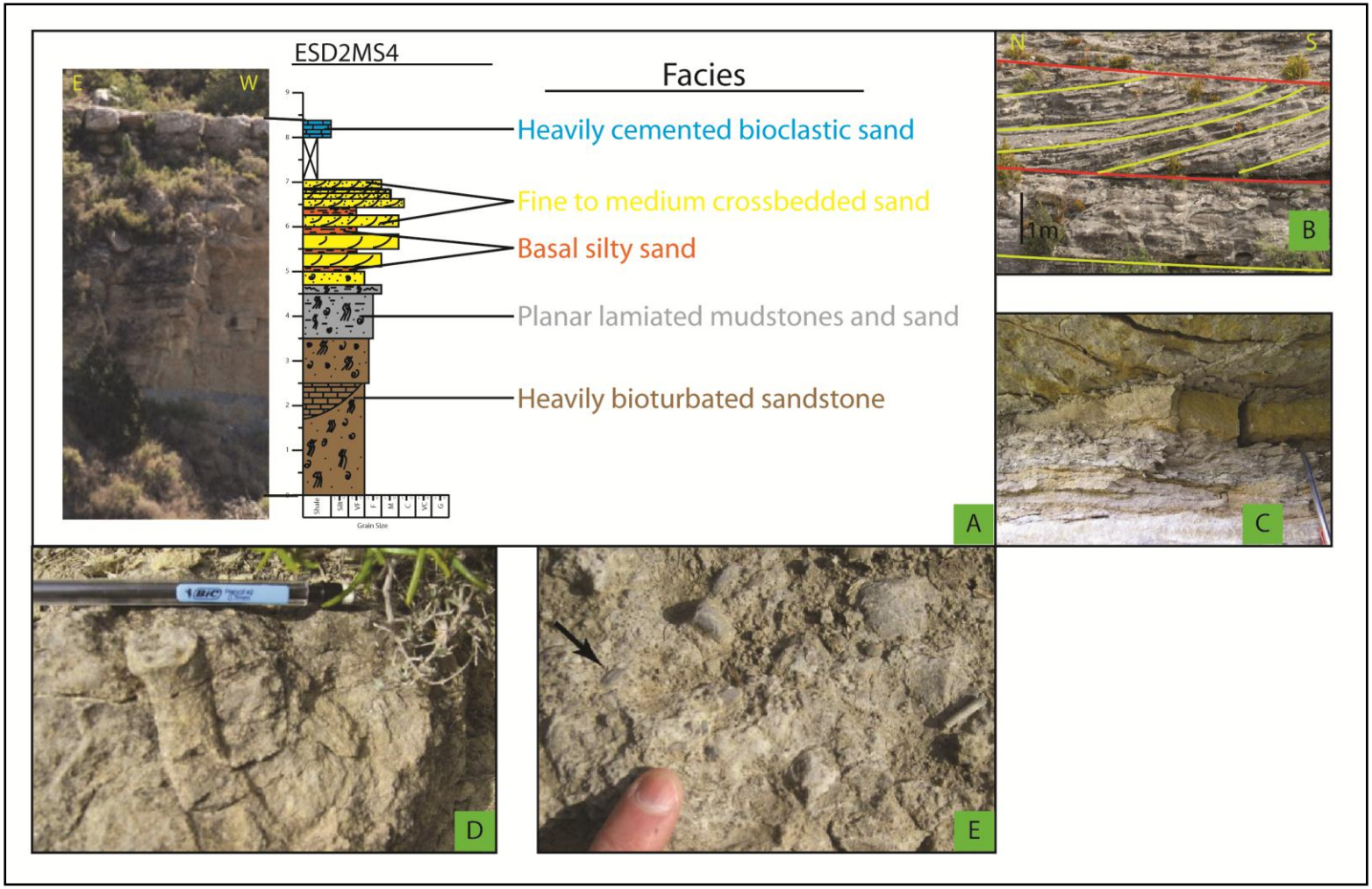

Figure 13: A) Type section with photo and the five different facies colored and labeled. B) Photo of crossbedded sandstone facies with foresets shown in yellow and master surfaces shown in red. C) Basal silty sand facies. D) *Psilonichus* burrow from the heavily bioturbated sandstone facies. E) Foraminifera from the heavily cemented bioclastic sandstone facies.

Measured Section Correlation

A correlation and resulting architectural model (Figure 14) was created based on the ten measured sections taken along a proximal (NE) to distal (SW) transect in the Isábena river valley. Using the fossiliferous, bioturbated layer as the base of the sand bar across the measured sections, a 2-D geologic model of the ESD2 sand bar was generated. The basal bioturbated layer is absent from some of the measured sections where there was limited outcrop exposure, and so it has been projected below the bottom in these situations. This layer belongs to the heavily bioturbated sandstone facies and makes up the toesets and lower foresets of the sand bar. It interfingers with the crossbedded sands in the middle and upper part of the sand body (see Figure 14).

Geologic Model

Based on the geologic data from measured sections and previous work in the area, a conceptual model was created to illustrate the paleoenvironment it which the Esdolomada 2 type sand bars were deposited (Figure 15). The Esdolomada sandstone is genetically related to a southwestwardly prograding delta to the northeast (Tinterri 2007). As this delta deposited sand onto the shelf in a shallow marine environment, the sands were reworked by tidal currents flowing northwest and southeast (with the dominant direction being northwest) and formed shore-oblique tidal sand bars. Master surface measurements indicates that the ESD2 sand bars were laterally accreting towards the south west while tidal currents formed cross-strata that were migrating towards the northwest. The extent of the clean sandstone facies indicate that ESD2 tidal bar is about 1000 m wide which is wider than Esdolomada1 tidal bar (1.5-2 km)

and has implications for the paleogeography since the width/length of the tidal bars correlate (Wood, 2004).

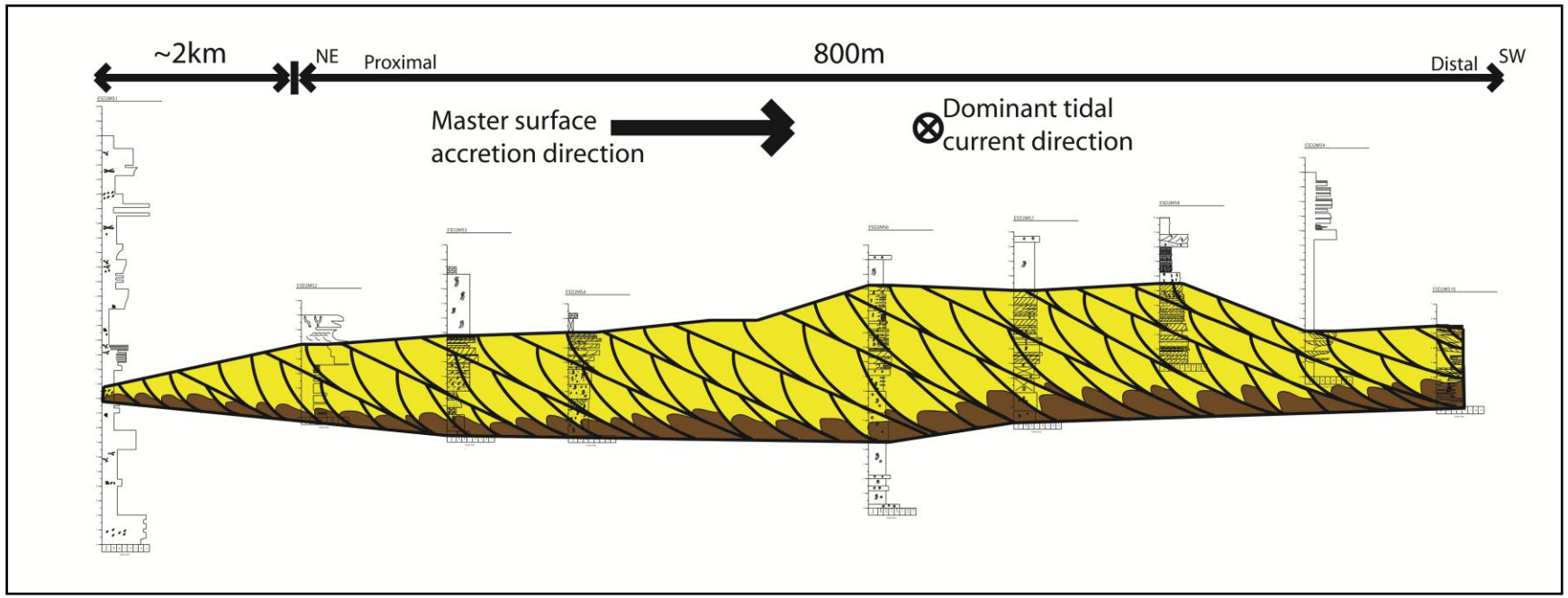

Figure 14: Schematic illustration of the tidal shelf bars lying just off the tip of the deltas on their landward side. See the location of the measured sections on Figure 9. The bars are elongated to the NW in the direction of strongest tidal flow, but migrate laterally to the SW through time. Yellow is the sandstone dominated facies (mostly cross-stratified sandstone) and brown are muddy, highly bioturbated facies.

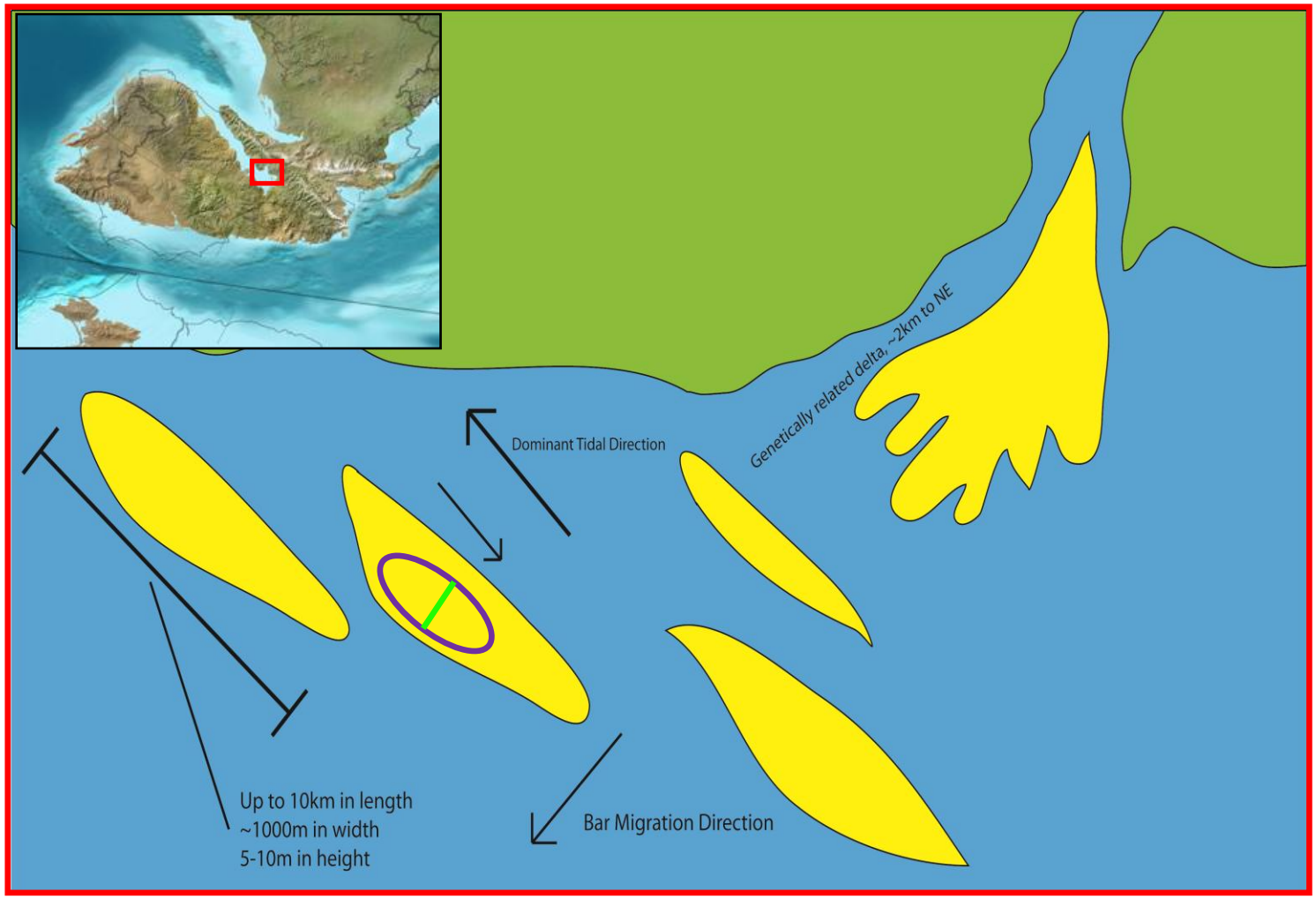

Figure 15: Blakey paleogeographic map (top left) showing Spain during the Eocene, with the location of ESD2 sand bar deposition highlighted in red. The larger illustration shows the interpreted depositional environment of the ESD2 sand bars and their dimensions. The purple oval represents the part of the sand bar being modeled. The SW-NE axis of the oval (green) represents the transect across which the first 9 measured sections were taken. Note: figure not to scale.

Chapter 5: Reservoir Model

Methods

Schlumberger's Petrel software was used to build a geologic facies model and porosity model of the Esdolomada 2 sand bar. The two models that were created are discussed below. The first step in modeling the ESD2 sand bar was to digitize the measured sections in Petrel, i.e. translating the geologic data into facies and assigning petrophysical data (Figures 16 and 19) so that Petrel could read the information as well logs. After digitizing all ten measured sections, the next step was to correlate key surfaces across the measured sections in order to constrain the geologic model. Top and bottom surfaces for the sand bar were created following the same correlation shown in Figure 14. After correlating the top and bottom across the sections, a single accretion surface with the dip of 10 degrees representing a master surface was created. The surface was created based on the geological model produced (Figure 14) and using the outcrop measurements of the master surfaces. The actual length of an ESD2 type sand bar has been interpreted to be up to 20km, but this is too large to model considering the data coverage. Therefore the next step was to create an ovoid boundary (roughly 2km in length 800m in width) representing a bar form to laterally constrain the data surrounding the wells. It is assumed that the central part of the bar that is being modeled is also the optimal area to target for drilling/production and therefore useful to build a reservoir model.

With the data laterally and vertically constrained, a 3-D grid was built to fill the space within the constraints that could be populated with interpolated data from the measured sections. Using the layering options in Petrel, the single master surface created previously was replicated to fill the reservoir with spacing between surfaces corresponding to field observations and geologic model. Next, the facies and petrophysical data were upscaled and then interpolated throughout the grid using Gaussian processes to create a 3-D facies model and porosity model (Figures 16 and 19). In order to constrain the porosity model, a "facies mask" was used to correct for some of the pitfalls inherent to interpolation.

Facies Model

For the sake of model building, i.e. in order to capture the more subtle changes in geologic heterogeneities, 11 facies were designated based on measured section data. Petrophysical data (porosity, vertical and horizontal permeability) was formulated from analogous facies at depth (Manzocchi et al., 2008). The 11 petrofacies and their petrophysical values are shown in the Table 2 on the following page.

Petrofacies	Porosity (%)	Kv (md)	Kh (md)	Color
Silt	0.05	0.05	0.05	
Very fine sand	0.15	1.3	55	
Medium cross bedded sand	0.25	1.95	90	
Fine cross bedded sand	0.18	1.5	60	
Bioturbated sand	0.12	1	40	
Bioturbated silty sand	0.09	0.8	30	
Thinly laminated sand	0.2	1.2	65	
Very coarse sand	0.3	2	100	
Bioclastic sand (heavily cemented)	0.1	1	20	
Limestone	0.07	0.6	10	
Shale	0.03	0.02	0.02	

Table 2: Table summarizing the petrofacies used in modeling and their associated colors and petrophysical values.

Because 9 of the 10 measured sections are uniformly spaced and represent the central part of an ESD2 bar, one measured section (ESD2MS1) has been omitted because of its distance (about 2km) away from the other sections. If this section were to be considered in the interpolation used to generate the model, it would introduce too much error.

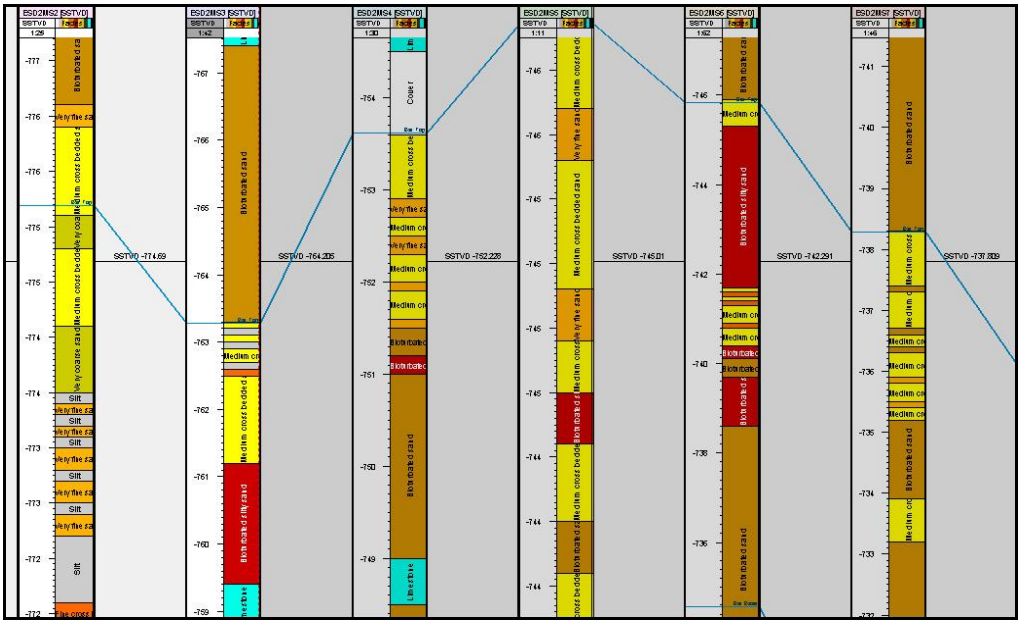

Figure 16: Digitized measured sections in Petrel showing facies and the correlated bar top surface. Note that the vertical scale of the sections is different.

The resultant facies model has a high degree of anisotropy in the northwest-southeast direction (perpendicular to master surfaces) and is far more continuous along the long axis of the sand bar (east-west oriented), which is parallel to master surfaces. As an oil reservoir, the ESD2 sand bar would be a favorable prospect as it has a high proportion of clean to moderately clean sand (Figures 17 and 18) and only has significant barriers to fluid flow perpendicular to master surfaces. In other words, the units will have a good connectivity in a NW-SE direction according to the facies model. The facies model also show some pinch outs along the bar such as the bioturbated silty sand (red on Figure 17). In the cutaway of the facies model (Figure 18), smaller scale heterogeneities are apparent.

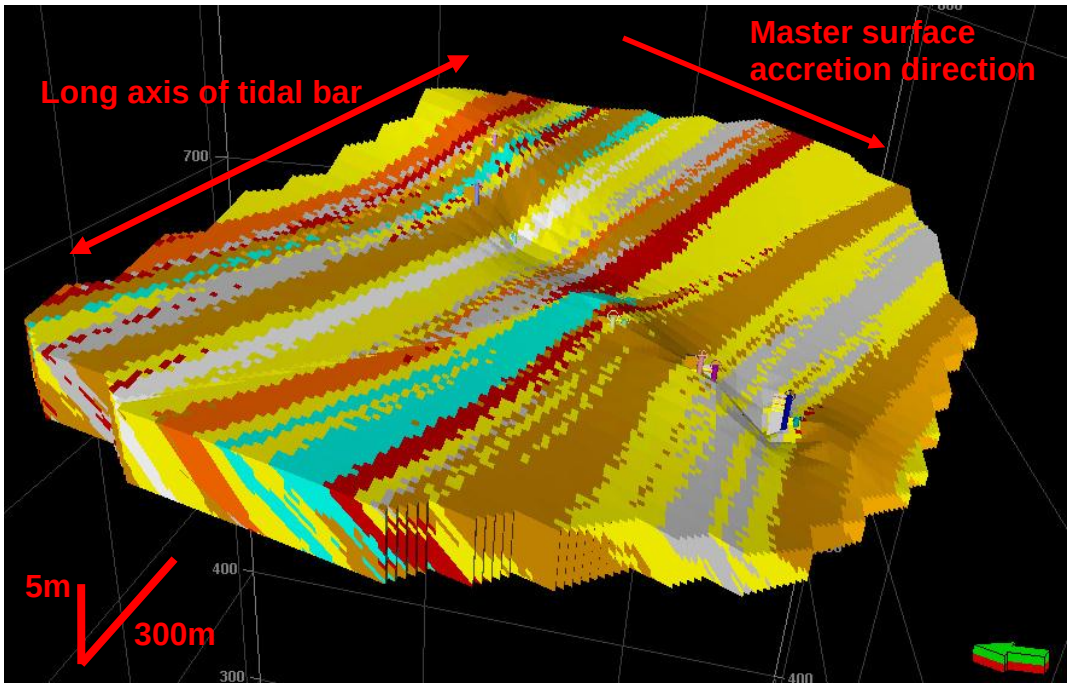

Figure 17: 3-D facies model of the Esdolomada 2 type sand bar shown with 10x vertical exaggeration. The orange and red facies indicate higher degrees of bioturbation, while the yellows are cleaner, crossbedded sands. Note that facies is continuous in a NW-SE direction.

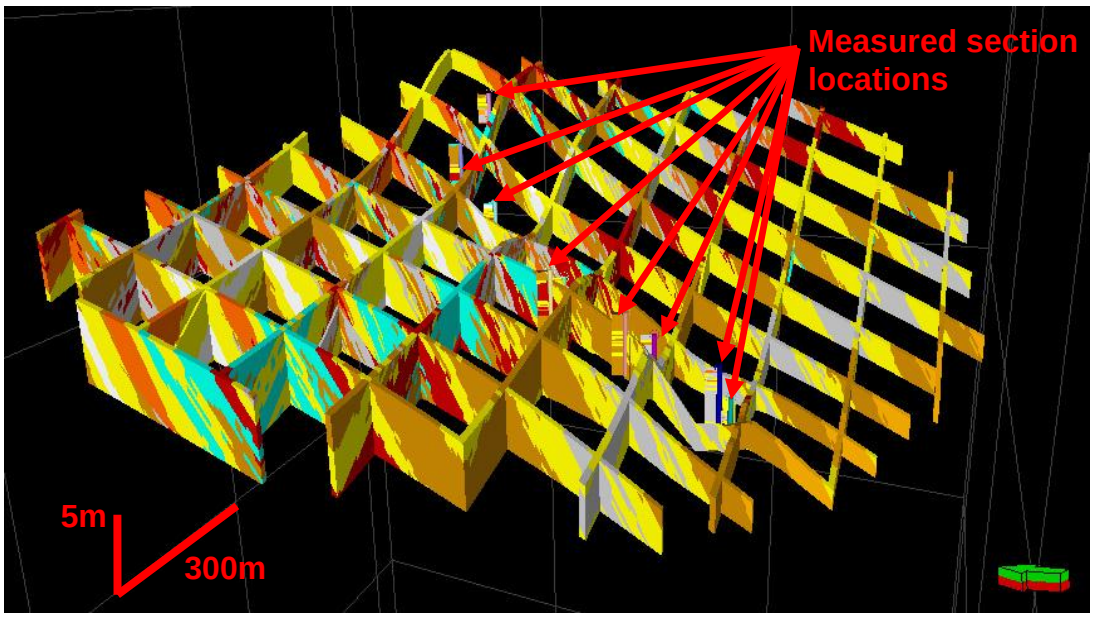

Figure 18: Cutaway view through the facies model.

Porosity Model

Using the upscaled porosity data from the measured section, a 3-D porosity model was generated to better understand the quality of the Esdolomada 2 sand bar as a reservoir (Figures 20 and 21). While a facies model offers a good view of the lithology in a discrete sense, it is not necessarily indicative of the distribution of petrophysical properties, chief among which is porosity. To constrain the porosity model further than Petrel can accomplish merely through interpolation, a “facies mask” was used so that Petrel would honor certain facies when interpolating porosity.

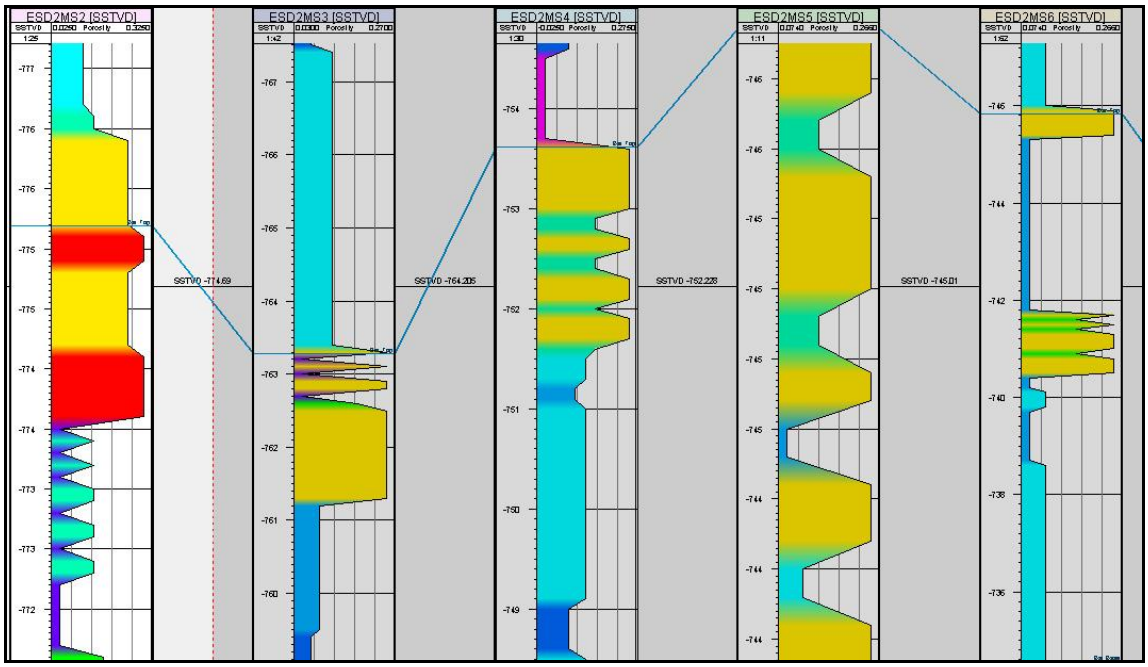

Figure 19: Porosity logs for five of the measured sections with the correlated bar top surface shown.

When interpolating a very thin, very low porosity facies (silt) adjacent to a much thicker high porosity facies (crossbedded sand), typical Gaussian

interpolation would cause the thin, low porosity facies to become “diluted” by the adjacent, thicker facies and the resultant model would have little to no trace of the thinner facies present. However, by using the calculator function in Petrel, “IF, THEN” statements can be assigned to certain facies to insure that Petrel honors these very thin, low porosity facies that are important to a reservoir model but would become obscured by typical interpolation techniques. This process is called “facies masking.”

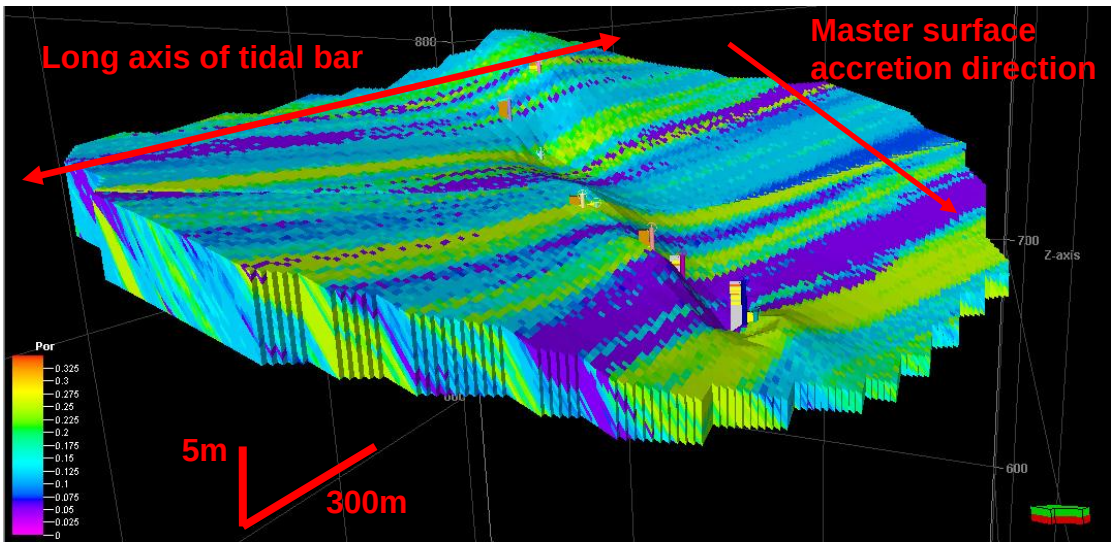

Figure 20: 3-D porosity model of the Esdolomada 2 type sand bar shown at 10x vertical exaggeration.

As with the facies model, the porosity model follows the same trends in anisotropy. The average porosity for the reservoir is around 15%, with the sandier streaks containing higher values of 25-30%, and the bioturbated, siltier facies containing the lower values (5% or less). Because of the high degree of lateral continuity along the long axis of the bar, the ESD2 reservoir and other analogous tidal sand bar systems would be best targeted for production by

drilling wells parallel to the long axis at regular intervals into the crossbedded sandstones.

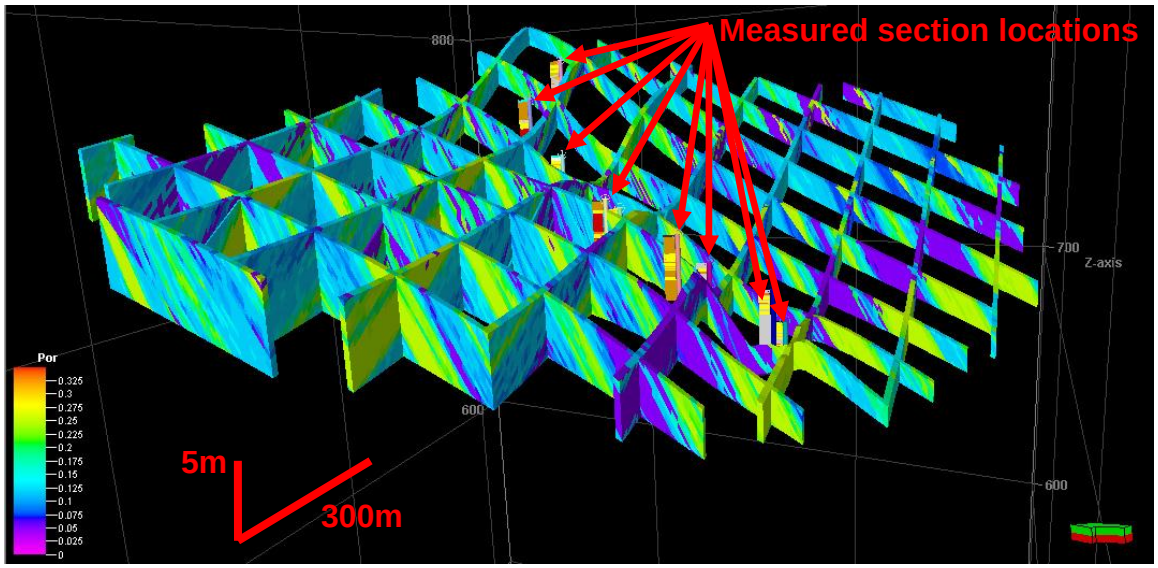

Figure 21: Cutaway view of the 3-D porosity model, shown at 10x vertical exaggeration.

Discussion

Interpretation of the Esdolomada 2 as a tidal bar formed in a marine environment was based on the facies (cross-strata with mud drapes) and trace marine fossil assemblages (Figure 13, see also measured sections in the appendix). This interpretation is similar to that of the first sandstone unit of the Esdolomada Member (Olariu et al., 2012), which was also recognized to be a tidal bar. The facies, paleocurrents, and the bar long axis orientation (northwest-southeast) are similar for both sandstone units. However, there are some differences regarding the dimensions. For instance, the Esdolomada 2 tidal bar is thicker (6-7m versus 5.5m for the Esdolomada 1). The Esdolomada 2 is also

less wide, about 1000m, compared with 1700m for the Esdolomada 1 (Olariu et al. 2012). The dimensional difference between Esdolomada 1 and Esdolomada 2 might be a general trend during transgression, but the large scale pattern during transgression was not studied. The distance of the Esdolomada 2 tidal bar from its coeval shoreline (tidal delta to the northeast) was about 2 km (Figure 15). This distance is similar to the interpreted distance for the coeval tidal delta of the Esdolomada 1 tidal bar (Olariu et al., 2012).

The reservoir model, built using the petrophysical properties of the interpreted depositional petrofacies (Figures 17 and 18), shows the reservoir units to be inclined in a clinoformal manner because of the presence of the large accretion surfaces and the facies distributions. The tidal facies is usually highly heterolithic with sandstone-mudstone beds apparently continuous at small scales but most probably discontinuous at medium and large scales (Figure 22 upper). The reservoir facies model of Esdolomada 2 (Figure 22 lower) incorporates small scale heterogeneities statistically, but is capturing the large scale variability (facies changes along accretion surfaces) with accuracy.

There are no published simulation flows through tidal bars reservoirs. However, the internal geometry of the Esdolomada 2 (large accretion surfaces from cleaner, cross-stratified sands to muddy sands) is similar to those of the shoreface clinoforms that were modeled by Jackson et al. (2009). The Esdolomada 2 reservoir is expected to drain similar to shoreface deposits (Figure 23), despite the scale differences.

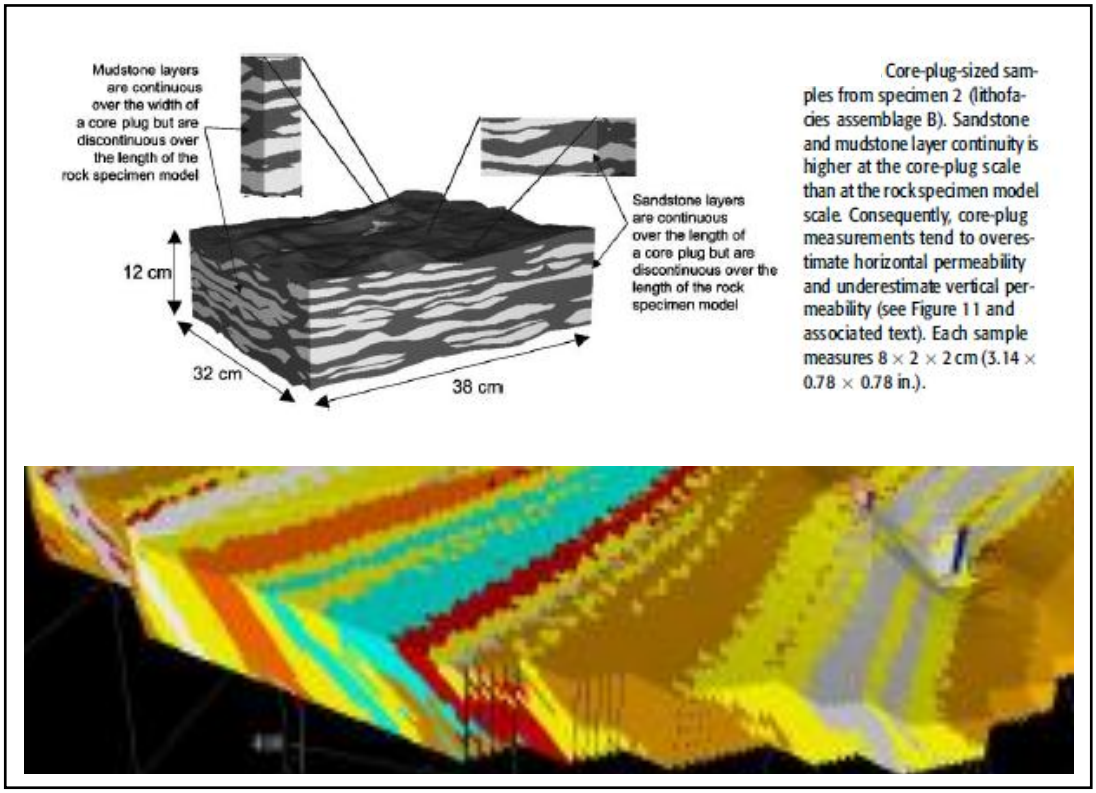

Figure 22: Comparison between tidal heterogeneities at small and medium scale (upper figure, from Jackson et al., 2005) and Esdolomada 2 large scale geometries (lower figure).

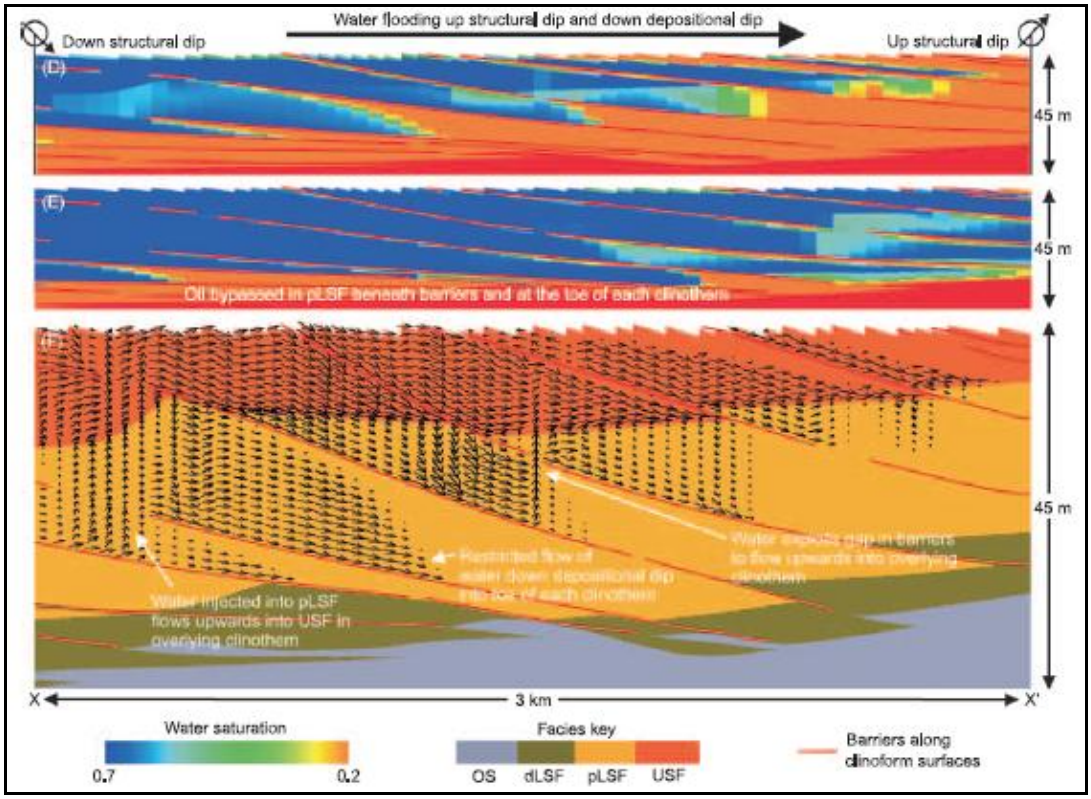

Figure 23: Reservoir model and flow simulation through shoreface clinoforms (from Jackson et al., 2009). Note that scale is significantly larger than Esdolomada 2 deposits but the geometries are similar.

Conclusions

The second sandstone unit of the Esdolomada Member of the Eocene Roda Formation in the Tremp-Graus Basin was interpreted as a tidal bar formed in a marine setting. The outcrop observations show that the tidal bar is about 4-5m thick and extends for about 1000m. The dominant tidal paleocurrents have a northwest-southeast orientation while the accretion surfaces within the tidal bar dip (accreted) toward the southwest. The Esdolomada 2 tidal bar is smaller than

the underlying Esdolomada 1 tidal bar, which was estimated to have a width of 1500-2000m.

The reservoir model of the Esdolomada 2 tidal bar shows that the facies follow the main heterogeneities (accretion surfaces) within the sandstone units. The facies are the main control for the reservoir porosities, and the Esdolomada 2 reservoir will most likely behave similar to a shoreface reservoir or any reservoir where clinoforms (or accretion surfaces) are present as flow barriers.

Appendix

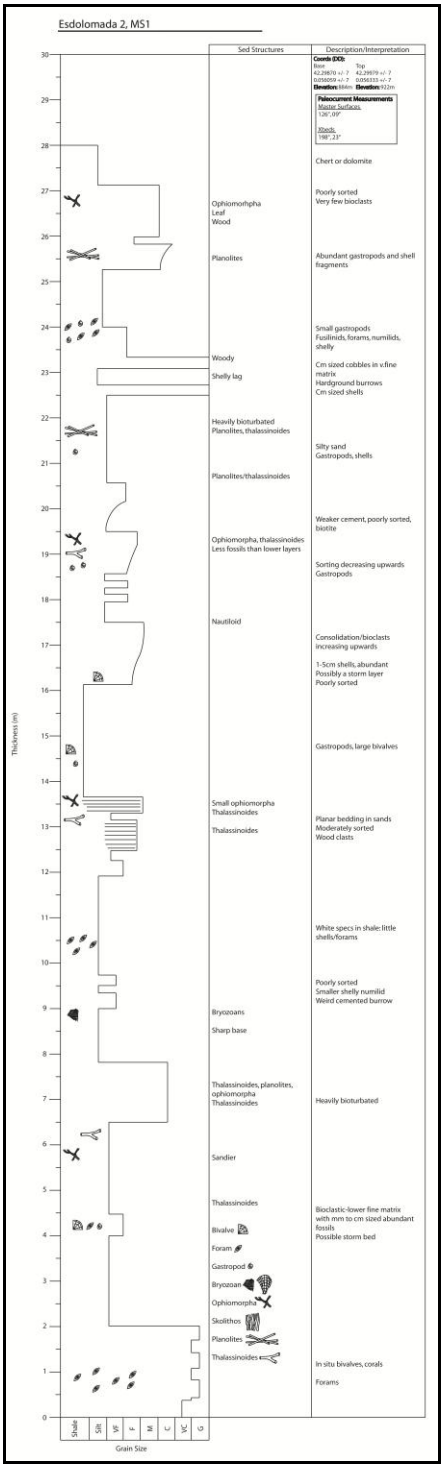

Figure 24: Esdolomada sandstone 2, measured section 1

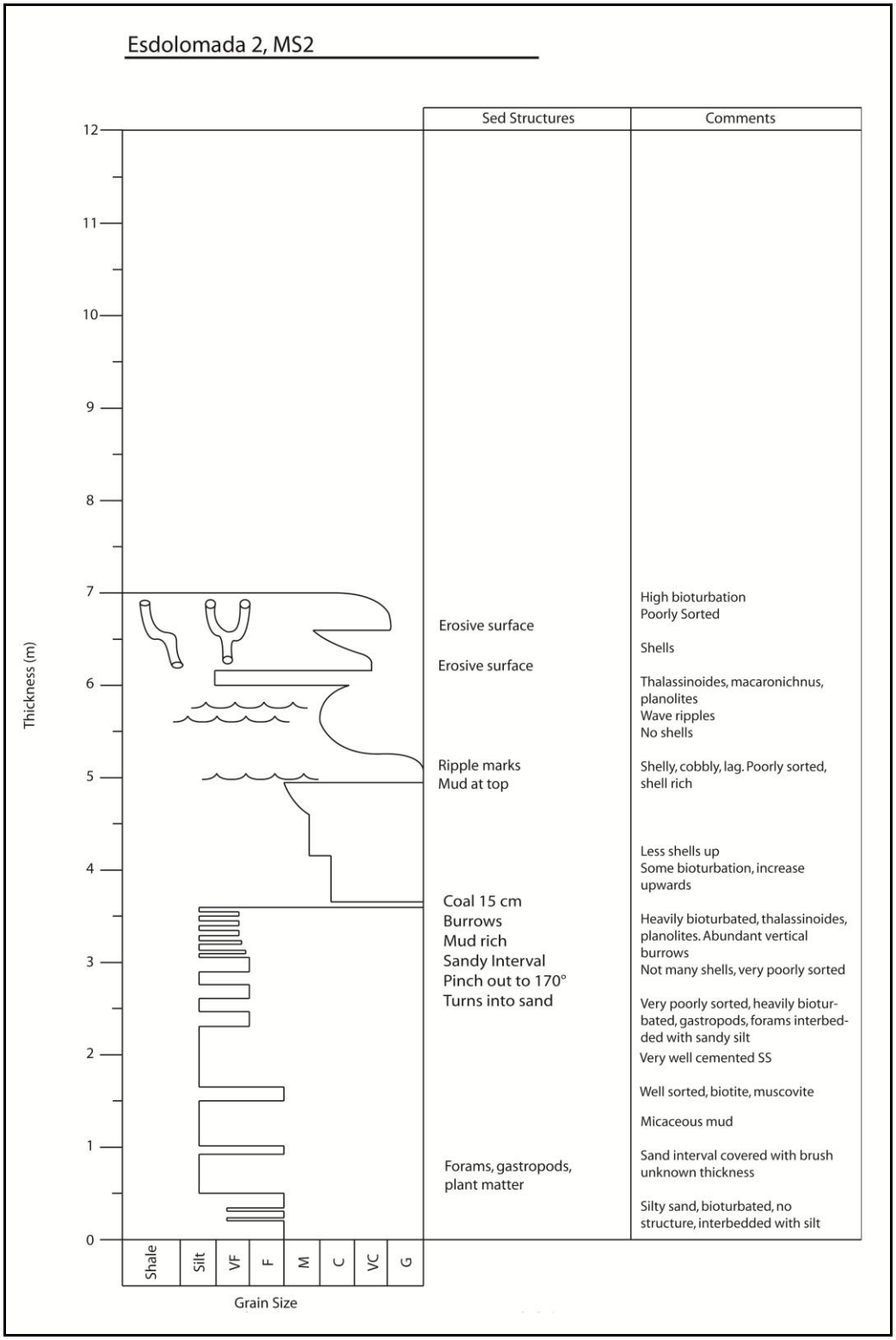

Figure 25: Esdolomada sandstone 2, measured section 2

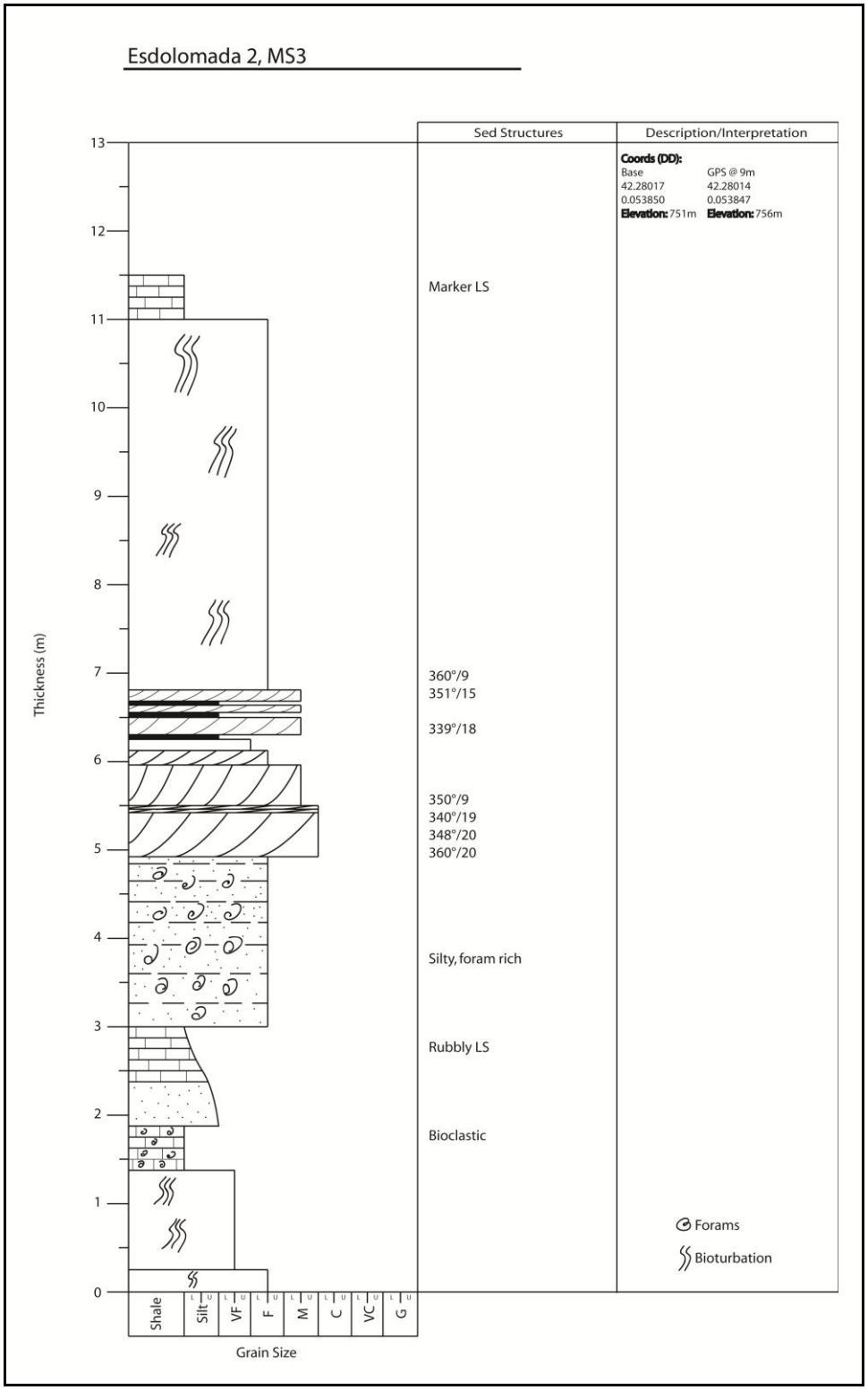

Figure 26: Esdolomada sandstone 2, measured section 3

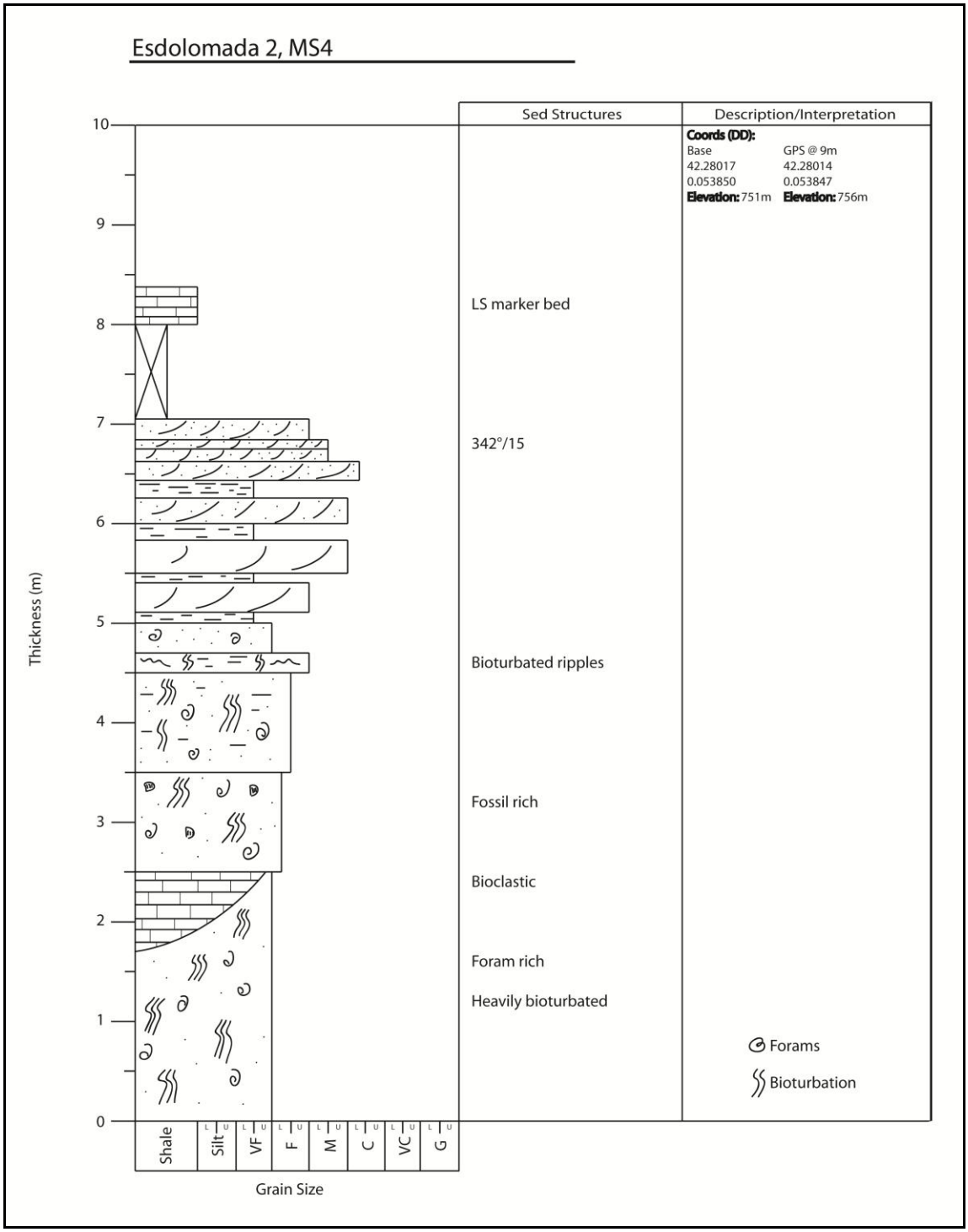

Figure 27: Esdolomada sandstone 2, measured section 4

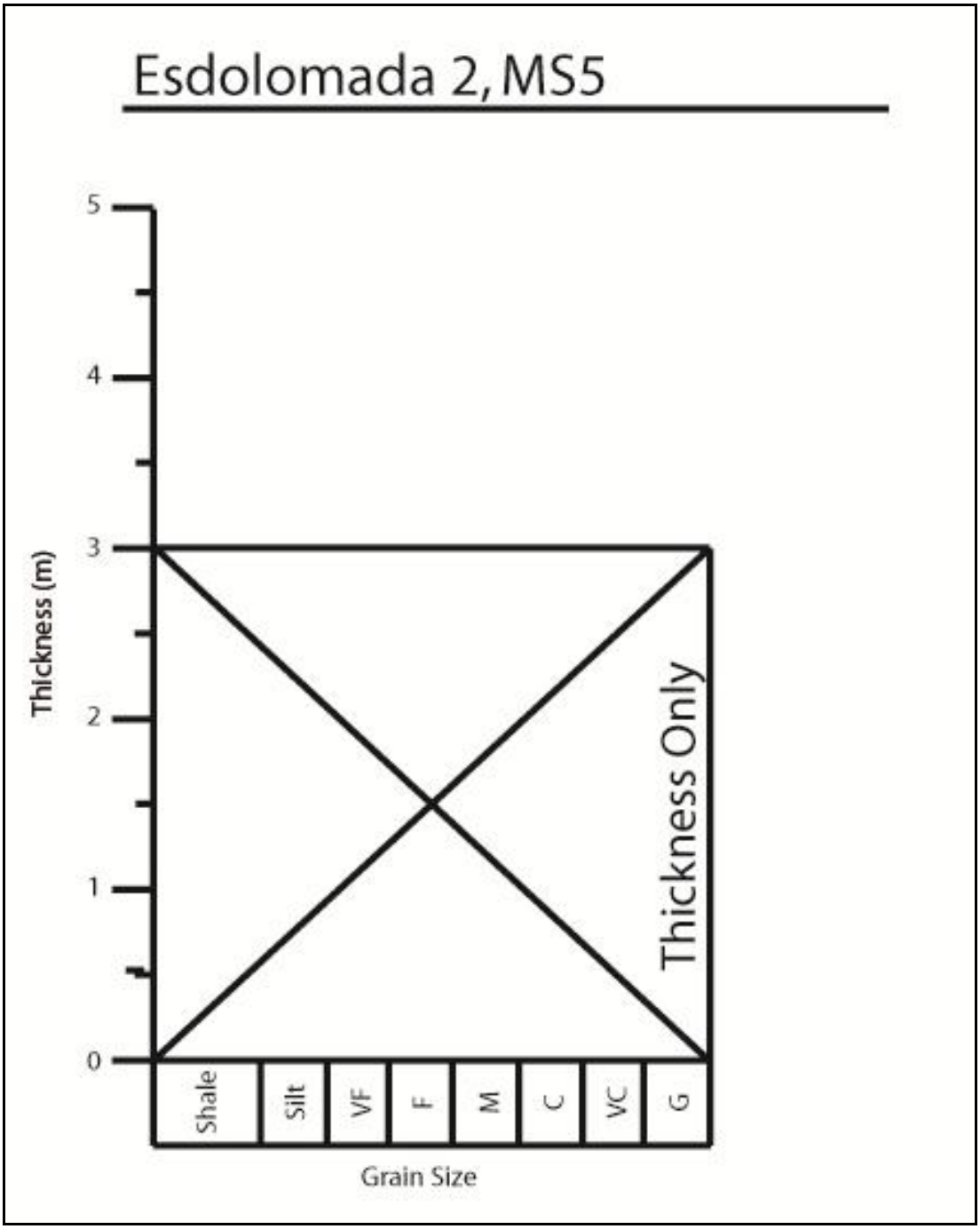

Figure 28: Esdolomada sandstone 2, measured section 5

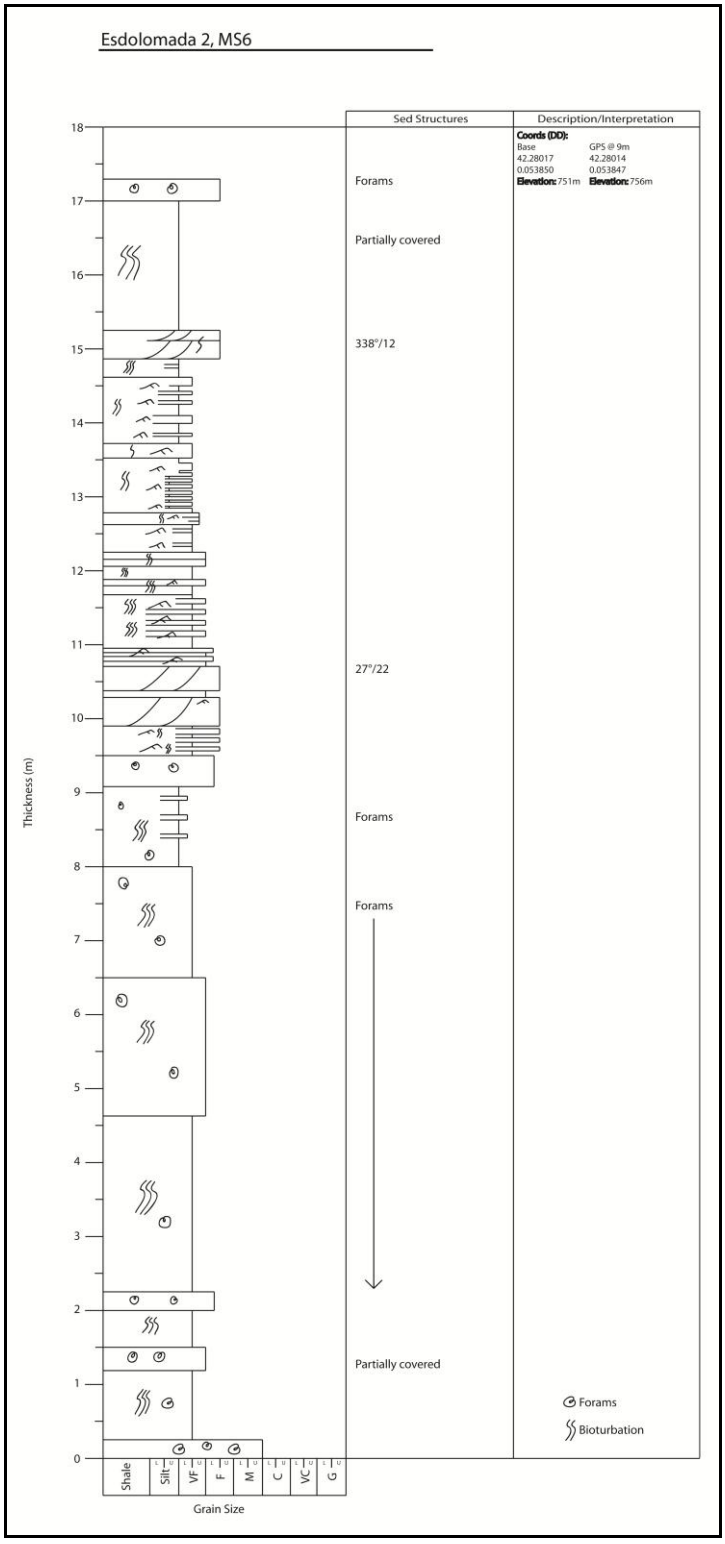

Figure 29: Esdolomada sandstone 2, measured section 6

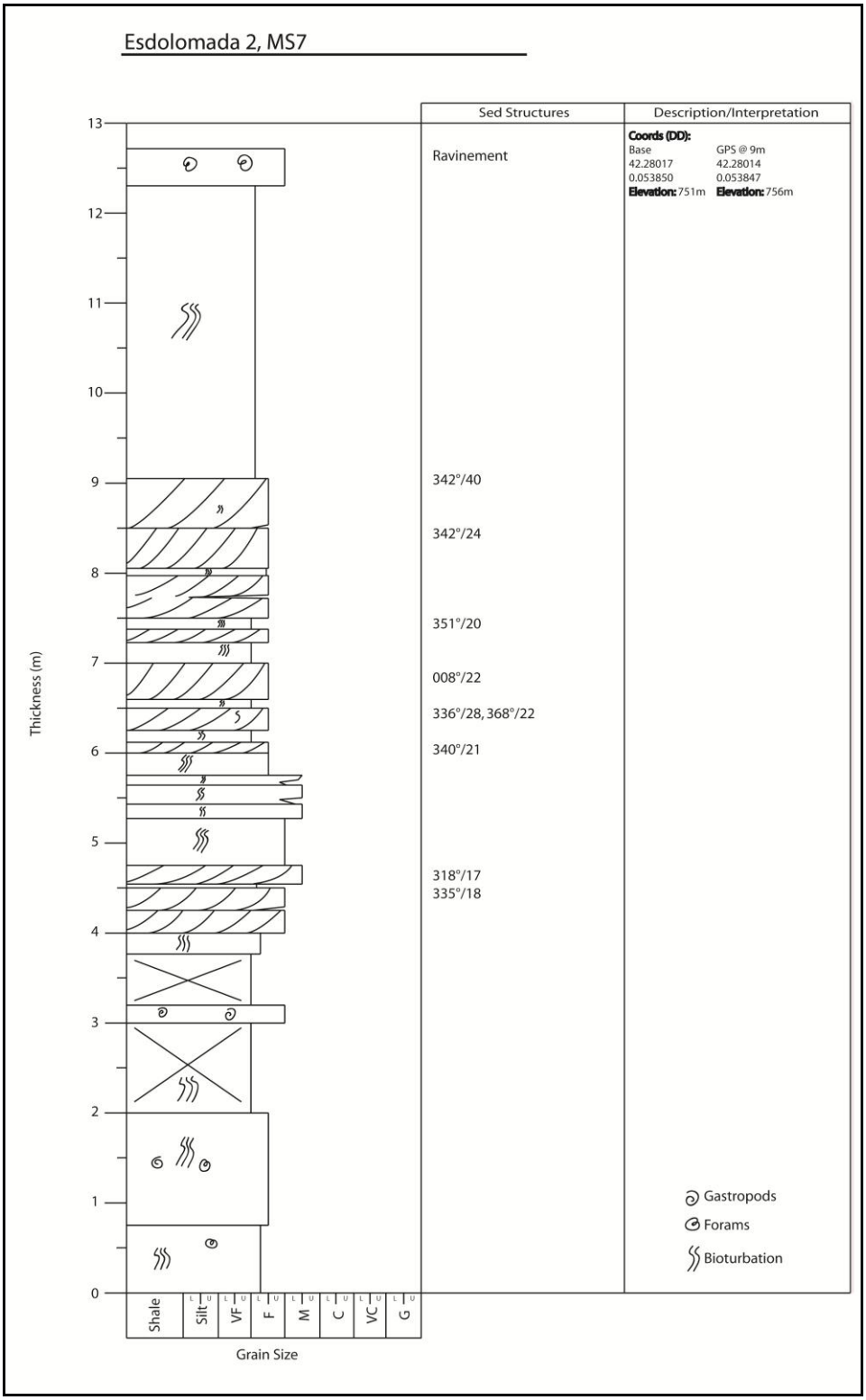

Figure 30: Esdolomada sandstone 2, measured section 7

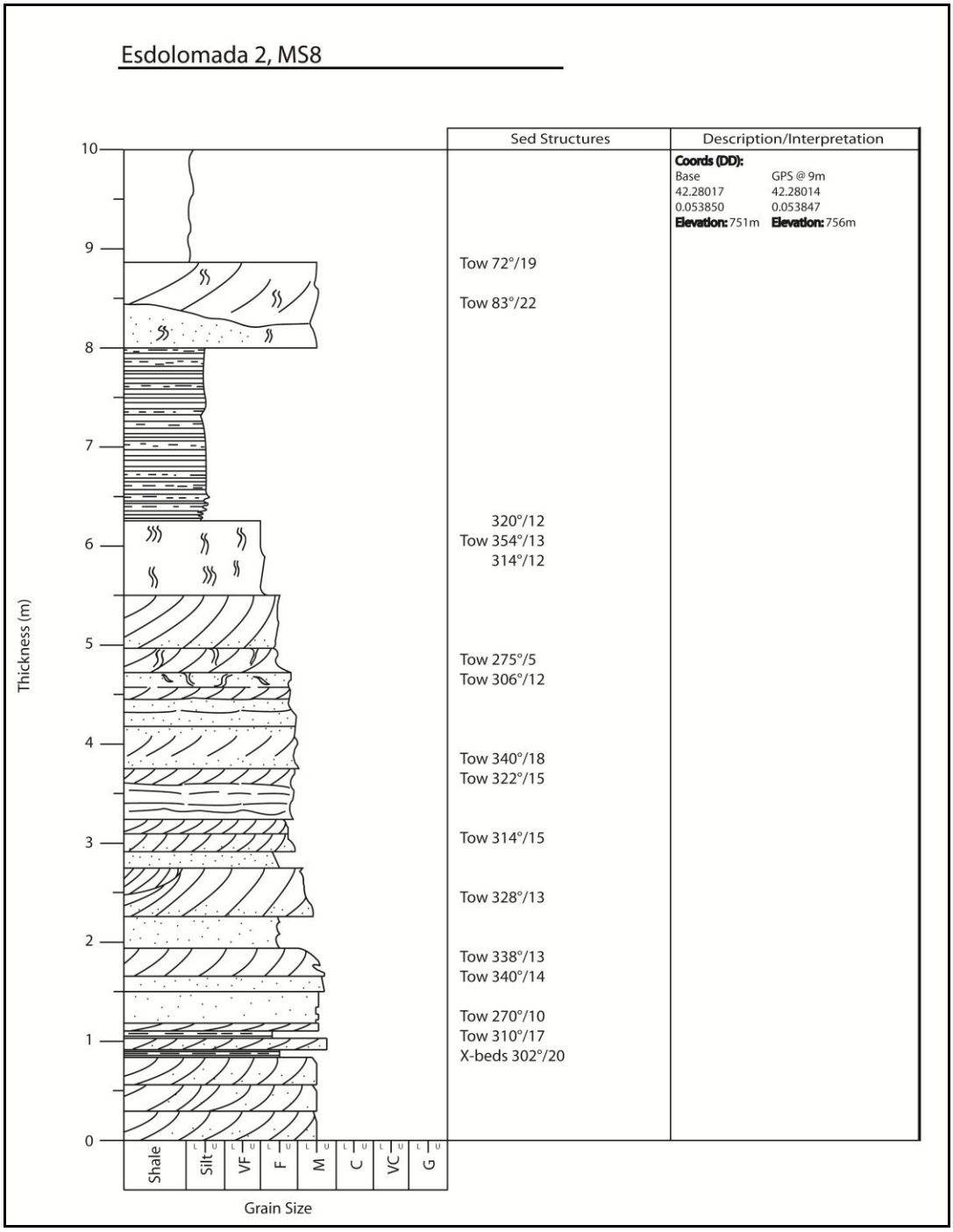

Figure 31: Esdolomada sandstone 2, measured section 8

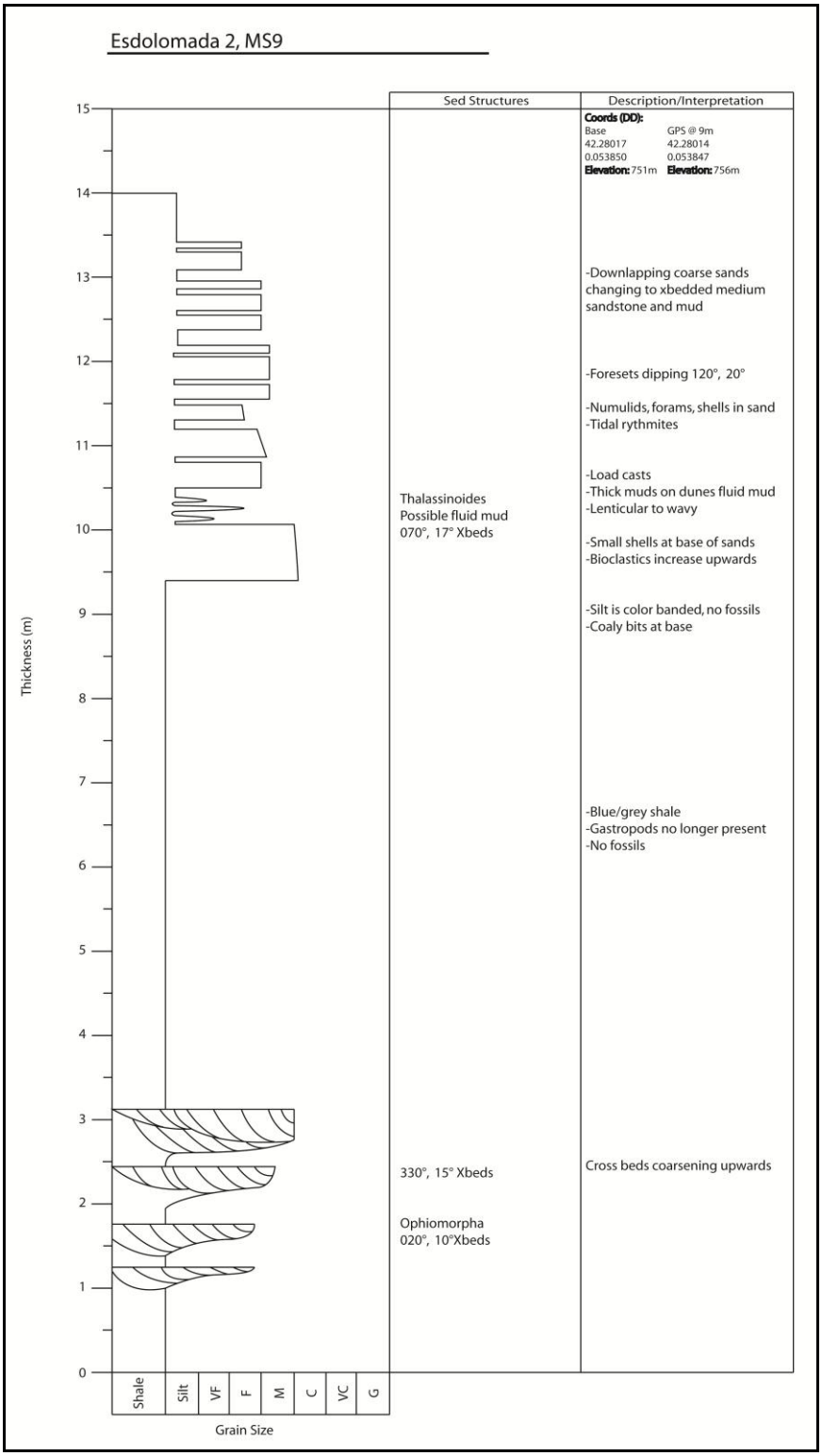

Figure 32: Esdolomada sandstone 2, measured section 9

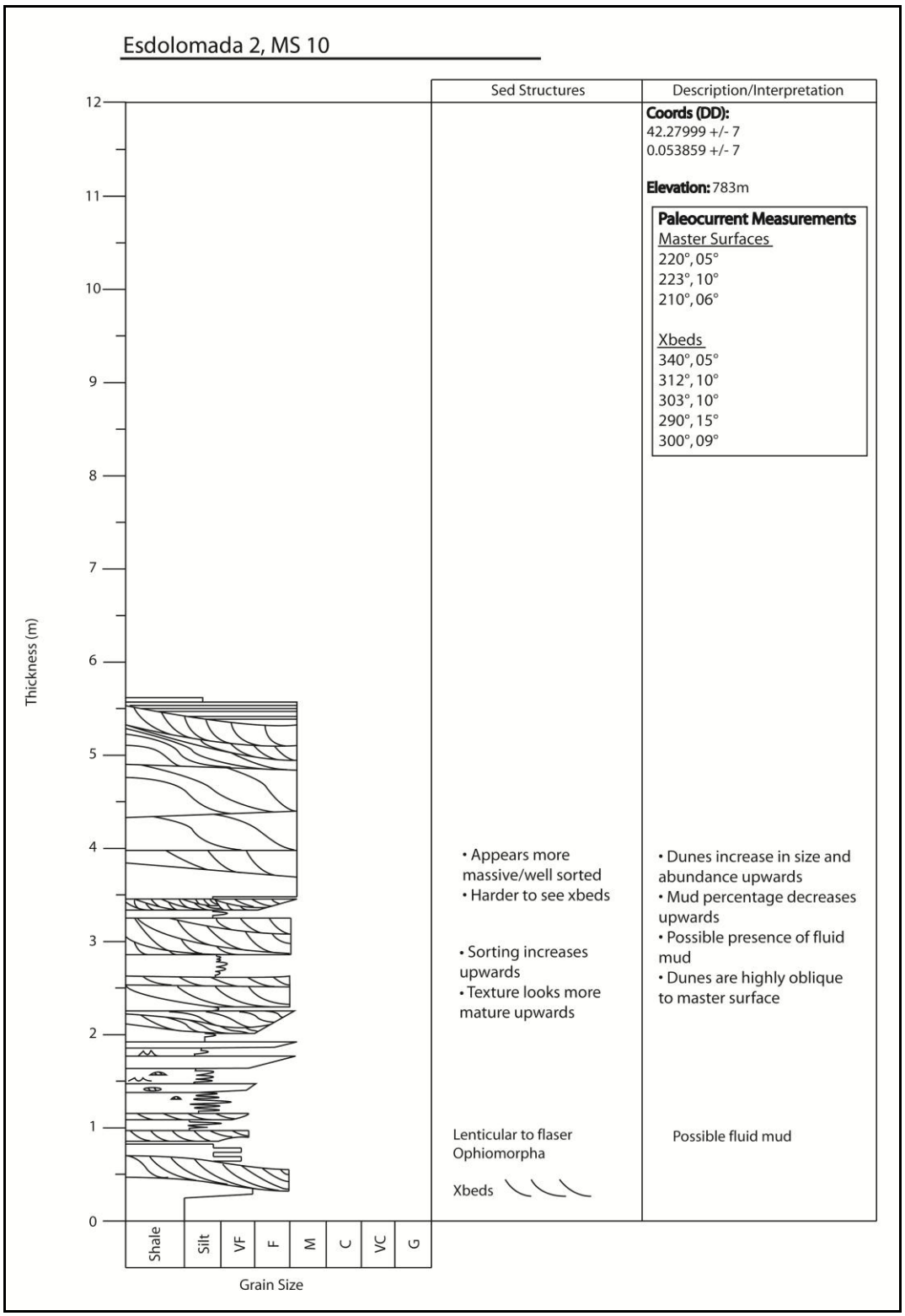

Figure 33: Esdolomada sandstone 2, measured section 10

References

Brønlund, S. 2010. Reservoir modeling of fluvial systems: An example from the Gulf of Thailand.

Campbell, W. G. 1990. Form and Style in Thesis Writing, a Manual of Style. Chicago: The University of Chicago Press.

Dalrymple, R.W. 1992. Facies Models; Response to Sea Level Change. Chapter 9: Tidal Depositional Systems. Geologic Association of Canada, St. Johns, NL, Canada. pp.195-218

Dalrymple, R.W. and Rhodes, R.N. 1995. Estuarine dunes and barforms, in Perillo, G.M.E., ed., Geomorphology and Sedimentology of Estuaries. Developments in Sedimentology, v. 53, p. 359-422.

Distal sectors of fluvial distributary systems: Examples from the Miocene Luna and Huesca Systems, northern Spain. Sedimentary Geology. 195. pp.55-73.

Enge, H.D. and Howell, J.A. 2010. Impact of deltaic clinothems on reservoir performance: Dynamic studies of reservoir analogs from the Ferron Sandstone Memberand Panther Tongue, Utah. AAPG Bulletin. V. 94, no.2. pp.139-161.

Enge, H.D., Buckley, S.J., Rotevatn, A., Howell, J.A. 2007. From outcrop to reservoir simulation model: Workflow and preocedures. Geosphere. V.3, no.6. pp.469-490.

Fisher, J.A., Nichols, G.J. and Waltham, D.A. 2007. Unconfined flow deposits in Jackson, M.D., Yoshida, S., Muggeridge, A.H., Johnson, H.D. 2005. Three- dimensional reservoir characterization and flow simulation of heterolithic tidal sandstones. AAPG Bulletin. V.89, no.4. pp.507-528.

López-Blanco, M., Marzo, M. and Muñoz, J.A. 2003. Low-amplitude, synsedimentary folding of a deltaic complex: Roda Sandstone (lower Eocene), South-Pyrenean Foreland Basin. Basin Research. 15. pp.73-95.

Manzocchi, T., Childs, C. and Walsh, J. J. 2010. Faults and fault properties in hydrocarbon flow models. Geofluids [Oxford], Vol. 10, Issue 1-2. pp. 94-113.

Manzocchi, T., et al. 2008. Sensitivity of the impact of geological uncertainty on production from faulted and unfaulted shallow-marine oil reservoirs; objectives and methods. Petroleum Geoscience, Vol. 14, Issue 1. pp. 3-15.

Molenaar, N. and Martinius, A.W. 1996. Fossiliferous intervals and sequence boundaries in shallow marine, fan-deltaic deposits (Early Eocene, southern Pyrenees, Spain). Palaeogeography, Palaeoclimatology, Palaeoecology. 121. pp.147-168.

Nio, S.D. and Yang, C.S. 1991. Sea-level fluctuations and the geometric variability of tide-dominated sandbodies. Sedimentary Geology. 70. pp.161-193.

Novakovic, D., C.D. White, R.M. Corbeanu, W.S. Hammon III, J.P. Bhattacharya, and G.A. McMechan, 2002, Hydraulic effects of shales in fluvial-deltaic deposits: Ground-penetrating radar, outcrop observations, geostatistics and three-dimensional flow modeling for the Ferron Sandstone, Utah: Mathematical Geology, v. 34, no. 7, p. 857–893.

Olariu, M.I., Olariu, C., Steel, R.J., Martinius, A.W., and Darlymple, R.W., (in press 2011), Anatomy of a laterally migrating tidal bar: Esdolomada Member, Roda Formation, Graus-Tremp Basin, Spain: Sedimentology, Sedimentolog, v. 59 356–378.

Pringle, J.K., Howell, J.A., Hodgetts, D., Westerman, A.R., and Hodgson, D.M., 2006, Virtual outcrop models of petroleum reservoir analogues: a review of the current state-of-the-art. First Break, v. 24, p. 33-42.

Tinterri, R. 2007. The Lower Eocene Roda Sandstone (South-Central Pyrenees): An Example of a Flood-Dominated River-Delta System in a Tectonically Controlled Basin. Rivista Italiana di Paleontologia e Stratigrafia, Vol. 113, Issue 2, pp.223-255.

Toricelli, S., Knezaurek, G. and Biffi, U. 2006. Sequence biostratigraphy and paleoenvironmental reconstruction in the Early Eocene Figols Group of the Tremp–Graus Basin (south-central Pyrenees, Spain). Palaeogeography, Palaeoclimatology, Palaeoecology. 232. pp.1–35.

Turabian, K. L. 1987. A Manual for Writers of Term Papers, Theses, and Dissertations. 5th ed. Chicago: The University of Chicago Press.

Valero-Garcés, B.L., Navas, A., Machín, J., Walling, D. 1999. Sediment sources and siltationin mountain reservoirs: a case study from the Central Spanish Pyrenees. Geomorphology. 28. p.23-41.

White, C.D., and Barton, M.D., 1999, Translating outcrop data to flow models, with applications to the Ferron Sandstone: Society of Petroleum Engineers Reservoir Evaluation and Engineering, v.2, no.4, p.341–350.

Wood, L. J. 2004. Predicting tidal sand reservoir architecture using data from modern and ancient depositional systems, in Integration of outcrop and modern analogs in reservoir modeling. AAPG Memoir 80. p. 45-66.